

## REPORT DOCUMENTATION PAGE

Form Approved OMB NO. 0704-0188

The public reporting burden for this collection of information is estimated to average 1 hour per response, including the time for reviewing instructions, searching existing data sources, gathering and maintaining the data needed, and completing and reviewing the collection of information. Send comments regarding this burden estimate or any other aspect of this collection of information, including suggestions for reducing this burden, to Washington Headquarters Services, Directorate for Information Operations and Reports, 1215 Jefferson Davis Highway, Suite 1204, Arlington VA, 22202-4302. Respondents should be aware that notwithstanding any other provision of law, no person shall be subject to any penalty for failing to comply with a collection of information if it does not display a currently valid OMB control number.

**PLEASE DO NOT RETURN YOUR FORM TO THE ABOVE ADDRESS.**

1. REPORT DATE (DD-MM-YYYY) 19-02-2014	2. REPORT TYPE Final Report	3. DATES COVERED (From - To) 15-Feb-2011 - 14-Oct-2015		
4. TITLE AND SUBTITLE <b>BIOINSPIRED, MOBILE ROBOTS WITH HIGH STABILITY, FUNCTIONALITY AND LOW COST: FINAL REPORT</b>		5a. CONTRACT NUMBER W911NF-11-1-0094		
		5b. GRANT NUMBER		
		5c. PROGRAM ELEMENT NUMBER 0620BK		
6. AUTHORS George M. Whitesides, Robert Wood		5d. PROJECT NUMBER		
		5e. TASK NUMBER		
		5f. WORK UNIT NUMBER		
7. PERFORMING ORGANIZATION NAMES AND ADDRESSES Harvard University 1350 Massachusetts Avenue Suite 600 Cambridge, MA 02138 -3846		8. PERFORMING ORGANIZATION REPORT NUMBER		
9. SPONSORING/MONITORING AGENCY NAME(S) AND ADDRESS (ES) U.S. Army Research Office P.O. Box 12211 Research Triangle Park, NC 27709-2211		10. SPONSOR/MONITOR'S ACRONYM(S) ARO		
		11. SPONSOR/MONITOR'S REPORT NUMBER(S) 59656-MS-DRP.10		
12. DISTRIBUTION AVAILABILITY STATEMENT Approved for Public Release; Distribution Unlimited				
13. SUPPLEMENTARY NOTES The views, opinions and/or findings contained in this report are those of the author(s) and should not be construed as an official Department of the Army position, policy or decision, unless so designated by other documentation.				
14. ABSTRACT This final report summarizes the evolution of our M3 project from the development and refinement of pneunet systems, prototyping and fabrication of soft robots, investigation of actuation, to combinations of hard and soft robots.				
15. SUBJECT TERMS soft robots, actuators, pneunet, locomotion, flexible, combustion				
16. SECURITY CLASSIFICATION OF: a. REPORT UU    b. ABSTRACT UU    c. THIS PAGE UU		17. LIMITATION OF ABSTRACT UU	15. NUMBER OF PAGES	19a. NAME OF RESPONSIBLE PERSON George Whitesides
				19b. TELEPHONE NUMBER 617-495-9430

## **Report Title**

BIOINSPIRED, MOBILE ROBOTS WITH HIGH STABILITY, FUNCTIONALITY AND LOW COST: FINAL REPORT

## **ABSTRACT**

This final report summarizes the evolution of our M3 project from the development and refinement of pneunet systems, prototyping and fabrication of soft robots, investigation of actuation, to combinations of hard and soft robots.

**Enter List of papers submitted or published that acknowledge ARO support from the start of the project to the date of this printing. List the papers, including journal references, in the following categories:**

**(a) Papers published in peer-reviewed journals (N/A for none)**

Received      Paper

- 02/19/2014 8.00 C. Majidi, R. F. Shepherd, R. K. Kramer, G. M. Whitesides, R. J. Wood. Influence of surface traction on soft robot undulation,  
The International Journal of Robotics Research, (10 2013): 1577. doi: 10.1177/0278364913498432
- 02/19/2014 9.00 Bobak Mosadegh, Aaron D. Mazzeo, Robert F. Shepherd, Stephen A. Morin, Unmukt Gupta, Idin Zhalehdoust Sani, David Lai, Shuichi Takayama, George M. Whitesides. Control of soft machines using actuators operated by a Braille display,  
Lab on a Chip, (01 2014): 189. doi: 10.1039/c3lc51083b
- 02/19/2014 7.00 Robert F. Shepherd, Adam A. Stokes, Rui M. D. Nunes, George M. Whitesides. Soft Machines That are Resistant to Puncture and That Self Seal,  
Advanced Materials, (12 2013): 6709. doi: 10.1002/adma.201303175
- 09/14/2012 1.00 A. D. Mazzeo, X. Chen, M. Wang, G. M. Whitesides, A. A. Stokes, R. F. Shepherd, F. Ilievski, W. Choi, S. A. Morin. From the Cover: Multigait soft robot,  
Proceedings of the National Academy of Sciences, (11 2011): 20400. doi: 10.1073/pnas.1116564108
- 09/14/2012 3.00 S. A. Morin, R. F. Shepherd, S. W. Kwok, A. A. Stokes, A. Nemirovski, G. M. Whitesides. Camouflage and Display for Soft Machines,  
Science, (08 2012): 828. doi: 10.1126/science.1222149
- 09/14/2012 2.00 Ramses V. Martinez, Carina R. Fish, Xin Chen, George M. Whitesides. Elastomeric Origami: Programmable Paper-Elastomer Composites as Pneumatic Actuators,  
Advanced Functional Materials, (04 2012): 1376. doi: 10.1002/adfm.201102978
- 10/09/2013 4.00 Ramses V. Martinez, Jamie L. Branch, Carina R. Fish, Lihua Jin, Robert F. Shepherd, Rui M. D. Nunes, Zhigang Suo, George M. Whitesides. Robotic Tentacles with Three-Dimensional Mobility Based on Flexible Elastomers,  
Advanced Materials, (01 2013): 205. doi: 10.1002/adma.201203002
- 10/09/2013 6.00 Adam A. Stokes, Robert F. Shepherd, Stephen A. Morin, Filip Ilievski, George M. Whitesides. A Hybrid Combining Hard and Soft Robots,  
Soft Robotics, (07 2013): 70. doi: 10.1089/soro.2013.0002
- 10/09/2013 5.00 Robert F. Shepherd, Adam A. Stokes, Jacob Freake, Jabulani Barber, Phillip W. Snyder, Aaron D. Mazzeo, Ludovico Cademartiri, Stephen A. Morin, George M. Whitesides. Using Explosions to Power a Soft Robot,  
Angewandte Chemie International Edition, (03 2013): 2892. doi: 10.1002/anie.201209540

**TOTAL: 9**

**Number of Papers published in peer-reviewed journals:**

---

**(b) Papers published in non-peer-reviewed journals (N/A for none)**

Received      Paper

**TOTAL:**

**Number of Papers published in non peer-reviewed journals:**

---

**(c) Presentations**

**Number of Presentations:** 0.00

---

**Non Peer-Reviewed Conference Proceeding publications (other than abstracts):**

Received      Paper

**TOTAL:**

**Number of Non Peer-Reviewed Conference Proceeding publications (other than abstracts):**

---

**Peer-Reviewed Conference Proceeding publications (other than abstracts):**

Received      Paper

**TOTAL:**

**Number of Peer-Reviewed Conference Proceeding publications (other than abstracts):**

---

**(d) Manuscripts**

Received      Paper

**TOTAL:**

**Number of Manuscripts:**

---

**Books**

Received      Paper

**TOTAL:**

## Patents Submitted

"SOFT ROBOTIC ACTUATORS" Chen, Xin; Choi, Won Jae; Ilievski, Filip; Kwok, Sen Wai; Martinez, Ramses V.; Mazzeo, Aaron D.; Morin, Stephen A.; Nie, Zhihong; Shepherd, Robert F.; Stokes, Adam A.; Whitesides, George M., PCT/US11/61720 filed 11/21/2011

"System and Methods for Actuating Soft Robotic Actuators", Cademartiri, Ludovico; Chen, Xin; Freake, Jacob; Morin, Stephen A.; Nunes, Rui; Shepherd, Robert F.; Stokes, Adam A.; Whitesides, George M., PCT/US2012/059226 filed 10/8/2012

"Apparatus, System, and Method for Providing Fabric Elastomer Composites as Pneumatic Actuators" Martinez, Ramses V.; Whitesides, George M., PCT/US13/28250 filed 2/28/2013

"FLEXIBLE ROBOTIC ACTUATORS" Kalb, William Bell; Mazzeo, Aaron D.; Morin, Stephen A.; Shepherd, Robert F.; Whitesides, George M., PCT/US13/22593 filed 1/22/2013

"APPARATUS, SYSTEMS, AND METHODS FOR ACTUATING PRESSURIZABLE CHAMBERS", Mosadegh, Bobak; Whitesides, George M., PCT/US13/66164 filed 10/22/2012

"Soft Bladder for Interabdominal Surgery", Mosadegh, Bobak; Shepherd, Robert F.; Whitesides, George M., 61/892,595 filed 11/29/2012

"SYSTEMS AND METHODS FOR PROVIDING FLEXIBLE ROBOTIC ACTUATORS", Branch, Jamie L.; Fish, Carina R.; Ilievski, Filip; Jin, Lihua; Martinez, Ramses V.; Morin, Stephen A.; Nunes, Rui; Shepherd, Robert F.; Suo, Zhigang; Stokes, Adam A.; Whitesides, George M., PCT/US13/32297 filed 3/15/2013

"Apparatus, Systems, and Methods for Modular Soft Robots", Kwok, Sen Wai; Morin, Stephen A.; Shepherd, Robert F.; Whitesides, George M., PCT/US13/51092 filed 7/18/2013

"Mechanically Programmed Soft Actuators with Conforming Sleeves", Galloway, Kevin C.; Wood, Robert 61/893,093 PENDING

"Low Strain Pneumatic Networks for Soft Robots", Mosadegh, Bobak; Shepherd, Robert F.; Whitesides, George M., 61/867,845 PENDING

"Magnetic Assembly of Soft Robots with Hard Components", Kwok, Sen Wai; Morin, Stephen A.; Mosadegh, Bobak; Shepherd, Robert F.; So, Ju-Hee; Whitesides, George M., 61/772,183 PENDING

## Patents Awarded

### Awards

Whitesides:

King Faisal International Prize for Science (2011)

F.A. Cotton Award (Texas ACS Section) (2011)

Honorary Doctor of Science, Aarhus University, Denmark (2011)

Honorary Doctor of Science, Université Libre de Bruxelles (Belgium, 2012)

Honorary Doctor of Science, Freie Universität Berlin (Germany, 2012)

Honorary Doctor of Science, State University of New York, Birmingham (2013)

Honorary Doctor of Science, University of Victoria, British Columbia (Canada, 2013)

Industrial Research Institute Gold Medal (2013)

### Graduate Students

NAME	PERCENT SUPPORTED	Discipline
Samuel Felton	1.00	
<b>FTE Equivalent:</b>	<b>1.00</b>	
<b>Total Number:</b>	<b>1</b>	

### Names of Post Doctorates

<u>NAME</u>	<u>PERCENT_SUPPORTED</u>
Carmel Majidi	1.00
Robert Shepherd	0.50
Adam Stokes	0.75
Stephen Morin	0.50
Xin Chen	0.50
Wonjae Choi	0.50
Ramses Martinez	0.30
Alex Nemiroski	0.25
Sen Wai Kwok	0.25
Wenjie Lan	0.50
Yigit Menguc	0.50
Michael Wehner	0.50
Rui Nunes	0.50
Josh Lessing	0.50
Alok Tayi	0.25
Bobak Mosadegh	0.50
Rebecca Kramer	0.50
<b>FTE Equivalent:</b>	<b>8.30</b>
<b>Total Number:</b>	<b>17</b>

### Names of Faculty Supported

<u>NAME</u>	<u>PERCENT_SUPPORTED</u>	National Academy Member
George M. Whitesides	0.10	Yes
Robert Wood	0.30	No
<b>FTE Equivalent:</b>	<b>0.40</b>	
<b>Total Number:</b>	<b>2</b>	

### Names of Under Graduate students supported

<u>NAME</u>	<u>PERCENT_SUPPORTED</u>	Discipline
Jakob Freake	1.00	
Jordan Mancuso	1.00	
Cornell Young	1.00	
Lawrence Chan	1.00	
Sophia Wennstedt	1.00	
Sangsun Kim	1.00	
<b>FTE Equivalent:</b>	<b>6.00</b>	
<b>Total Number:</b>	<b>6</b>	

### **Student Metrics**

This section only applies to graduating undergraduates supported by this agreement in this reporting period

The number of undergraduates funded by this agreement who graduated during this period: ..... 0.00

The number of undergraduates funded by this agreement who graduated during this period with a degree in science, mathematics, engineering, or technology fields:..... 0.00

The number of undergraduates funded by your agreement who graduated during this period and will continue to pursue a graduate or Ph.D. degree in science, mathematics, engineering, or technology fields:..... 0.00

Number of graduating undergraduates who achieved a 3.5 GPA to 4.0 (4.0 max scale):..... 0.00

Number of graduating undergraduates funded by a DoD funded Center of Excellence grant for Education, Research and Engineering:..... 0.00

The number of undergraduates funded by your agreement who graduated during this period and intend to work for the Department of Defense ..... 0.00

The number of undergraduates funded by your agreement who graduated during this period and will receive scholarships or fellowships for further studies in science, mathematics, engineering or technology fields:..... 0.00

### **Names of Personnel receiving masters degrees**

NAME

**Total Number:**

### **Names of personnel receiving PhDs**

NAME

**Total Number:**

### **Names of other research staff**

<u>NAME</u>	<u>PERCENT SUPPORTED</u>
T.J. Martin	0.25
<b>FTE Equivalent:</b>	<b>0.25</b>
<b>Total Number:</b>	<b>1</b>

### **Sub Contractors (DD882)**

## Inventions (DD882)

### **5 Apparatus, System, and Method for Providing Fabric Elastomer Composites as Pneumatic Actuators**

Patent Filed in US? (5d-1) Y

Patent Filed in Foreign Countries? (5d-2) N

Was the assignment forwarded to the contracting officer? (5e) Y

Foreign Countries of application (5g-2):

5a: George M. Whitesides

5f-1a: Harvard University

5f-c: 12 Oxford Street

Cambridge MA 02138

5a: Ramses Martinez

5f-1a: Harvard University

5f-c: 12 Oxford Street

Cambridge MA 02138

### **5 APPARATUS, SYSTEMS, AND METHODS FOR ACTUATING PRESSURIZABLE CHAMBERS**

Patent Filed in US? (5d-1) Y

Patent Filed in Foreign Countries? (5d-2) N

Was the assignment forwarded to the contracting officer? (5e) Y

Foreign Countries of application (5g-2):

5a: Bobak Mosadegh

5f-1a: Harvard University

5f-c: 12 Oxford Street

Cambridge MA 02138

5a: George M. Whitesides

5f-1a: Harvard University

5f-c: 12 Oxford Street

Cambridge MA 02138

### **5 Apparatus, Systems, and Methods for Modular Soft Robots**

Patent Filed in US? (5d-1) Y

Patent Filed in Foreign Countries? (5d-2) N

Was the assignment forwarded to the contracting officer? (5e) Y

Foreign Countries of application (5g-2):

5a: Robert Shepherd

5f-1a: Harvard University

5f-c: 12 Oxford Street

Cambridge MA 02138

5a: Stephen Morin

5f-1a: Harvard University

5f-c: 12 Oxford Street

Cambridge

MA 02138

5a: Sen Wai Kwok

5f-1a: Harvard University

5f-c: 12 Oxford Street

Cambridge

MA 02138

5a: George M. Whitesides

5f-1a: Harvard University

5f-c: 12 Oxford Street

Cambridge

MA 02138

## 5 FLEXIBLE ROBOTIC ACTUATORS

Patent Filed in US? (5d-1) Y

Patent Filed in Foreign Countries? (5d-2) N

Was the assignment forwarded to the contracting officer? (5e) Y

Foreign Countries of application (5g-2):

5a: George M. Whitesides

5f-1a: Harvard University

5f-c: 12 Oxford Street

Cambridge

MA 02138

5a: Aaron D Mazzeo

5f-1a: Harvard University

5f-c: 12 Oxford Street

Cambridge

MA 02138

5a: William B Kalb

5f-1a: Harvard University

5f-c: 12 Oxford Street

Cambridge

MA 02138

5a: Robert Shepherd

5f-1a: Harvard University

5f-c: 12 Oxford Street

Cambridge

MA 02138

5a: Stephen Morin

5f-1a: Harvard University

5f-c: 12 Oxford Street

Cambridge

MA 02138

## **5 Low Strain Pneumatic Networks for Soft Robots**

Patent Filed in US? (5d-1) Y

Patent Filed in Foreign Countries? (5d-2) N

Was the assignment forwarded to the contracting officer? (5e) Y

Foreign Countries of application (5g-2):

5a: Robert Shepherd

5f-1a: Harvard University

5f-c: 12 Oxford Street

Cambridge MA 02138

5a: Bobak Mosadegh

5f-1a: Harvard University

5f-c: 12 Oxford Street

Cambridge MA 02138

5a: George M. Whitesides

5f-1a: Harvard University

5f-c: 12 Oxford Street

Cambridge MA 02138

## **5 Magnetic Assembly of Soft Robots with Hard Components**

Patent Filed in US? (5d-1) Y

Patent Filed in Foreign Countries? (5d-2) N

Was the assignment forwarded to the contracting officer? (5e) Y

Foreign Countries of application (5g-2):

5a: Ju-Hee So

5f-1a: Harvard University

5f-c: 12 Oxford Street

Cambridge MA 02138

5a: George M. Whitesides

5f-1a: Harvard University

5f-c: 12 Oxford Street

Cambridge MA 02138

5a: Robert Shepherd

5f-1a: Harvard University

5f-c: 12 Oxford Street

Cambridge MA 02138

5a: Bobak Mosadegh

5f-1a: Harvard University

5f-c: 12 Oxford Street

Cambridge MA 02138

5a: Stephen Morin

5f-1a: Harvard University

5f-c: 12 Oxford Street

Cambridge

MA 02138

5a: Sen Wai Kwok

5f-1a: Harvard University

5f-c: 12 Oxford Street

Cambridge

MA 02138

## 5 Mechanically Programmed Soft Actuators with Conforming Sleeves

Patent Filed in US? (5d-1) Y

Patent Filed in Foreign Countries? (5d-2) N

Was the assignment forwarded to the contracting officer? (5e) Y

Foreign Countries of application (5g-2):

5a: Kevin Galloway

5f-1a: Harvard University

5f-c: 60 Oxford Street

Cambridge

MA 02138

5a: Robert Wood

5f-1a: Harvard University

5f-c: 60 Oxford Street

Cambridge

MA 02138

## 5 PROGRAMMABLE PAPER-ELASTOMER COMPOSITES AS PNEUMATIC ACTUATORS

Patent Filed in US? (5d-1) Y

Patent Filed in Foreign Countries? (5d-2) N

Was the assignment forwarded to the contracting officer? (5e) Y

Foreign Countries of application (5g-2):

5a: George M. Whitesides

5f-1a: Harvard University

5f-c: 12 Oxford Street

Cambridge

MA 02138

5a: Ramses Martinez

5f-1a: Harvard University

5f-c: 12 Oxford Street

Cambridge

MA 02138

## **5 Soft Bladder for Interabdominal Surgery**

Patent Filed in US? (5d-1) Y

Patent Filed in Foreign Countries? (5d-2) N

Was the assignment forwarded to the contracting officer? (5e) Y

Foreign Countries of application (5g-2):

5a: Bobak Mosadegh

5f-1a: Harvard University

5f-c: 12 Oxford Street

Cambridge MA 02138

5a: Robert Shepherd

5f-1a: Harvard University

5f-c: 12 Oxford Street

Cambridge MA 02138

5a: George M. Whitesides

5f-1a: Harvard University

5f-c: 12 Oxford Street

Cambridge MA 02138

## **5 SOFT ROBOTIC ACTUATORS**

Patent Filed in US? (5d-1) Y

Patent Filed in Foreign Countries? (5d-2) N

Was the assignment forwarded to the contracting officer? (5e) Y

Foreign Countries of application (5g-2):

5a: Xin Chen

5f-1a: Harvard University

5f-c: 12 Oxford Street

Cambridge MA 02138

5a: Won Jae Choi

5f-1a: Harvard University

5f-c: 12 Oxford Street

Cambridge MA 02138

5a: Sen Wai Kwok

5f-1a: Harvard University

5f-c: 12 Oxford Street

Cambridge MA 02138

5a: Adam Stokes

5f-1a: Harvard University

5f-c: 12 Oxford Street

Cambridge MA 02138

5a: George M. Whitesides

5f-1a: Harvard University

5f-c: 12 Oxford Street

Cambridge MA 02138

5a: Ludovico Cademartiri

5f-1a: Harvard University

5f-c: 12 Oxford Street

Cambridge MA 02138

5a: Rui Nunes

5f-1a: Harvard University

5f-c: 12 Oxford Street

Cambridge MA 02138

5a: Filip Ilievski

5f-1a: Harvard University

5f-c: 12 Oxford Street

Cambridge MA 02138

5a: Zhihong Nie

5f-1a: Harvard University

5f-c: 12 Oxford Street

Cambridge MA 02138

5a: Ramses Martinez

5f-1a: Harvard University

5f-c: 12 Oxford Street

Cambridge MA 02138

5a: Aaron Mazzeo

5f-1a: Harvard University

5f-c: 12 Oxford Street

Cambridge MA 02138

5a: Robert Shepherd

5f-1a: Harvard University

5f-c: 12 Oxford Street

Cambridge MA 02138

5a: Stephen Morin

5f-1a: Harvard University

5f-c: 12 Oxford Street

Cambridge MA 02138

## 5 System and Methods for Actuating Soft Robotic Actuators

Patent Filed in US? (5d-1) Y

Patent Filed in Foreign Countries? (5d-2) N

Was the assignment forwarded to the contracting officer? (5e) Y

Foreign Countries of application (5g-2):

5a: Rui Nunes

5f-1a: Harvard University

5f-c: 12 Oxford Street

Cambridge MA 02138

5a: Robert Shepherd

5f-1a: Harvard University

5f-c: 12 Oxford Street

Cambridge MA 02138

5a: Adam Stokes

5f-1a: Harvard University

5f-c: 12 Oxford Street

Cambridge MA 02138

5a: George M. Whitesides

5f-1a: Harvard University

5f-c: 12 Oxford Street

Cambridge MA 02138

5a: Jacob Freake

5f-1a: Harvard University

5f-c: 12 Oxford Street

Cambridge MA 02138

5a: Stephen Morin

5f-1a: Harvard University

5f-c: 12 Oxford Street

Cambridge MA 02138

5a: Ludovico Cademartiri

5f-1a: Harvard University

5f-c: 12 Oxford Street

Cambridge MA 02138

5a: Xin Chen

5f-1a: Harvard University

5f-c: 12 Oxford Street

Cambridge MA 02138

## **5 SYSTEMS AND METHODS FOR PROVIDING FLEXIBLE ROBOTIC ACTUATORS**

Patent Filed in US? (5d-1) Y

Patent Filed in Foreign Countries? (5d-2) N

Was the assignment forwarded to the contracting officer? (5e) Y

Foreign Countries of application (5g-2):

5a: Adam Stokes

5f-1a: Harvard University

5f-c: 12 Oxford Street

Cambridge MA 02138

5a: Carina Fish

5f-1a: Harvard University

5f-c: 12 Oxford Street

Cambridge MA 02138

5a: Jamie Branch

5f-1a: Harvard University

5f-c: 12 Oxford Street

Cambridge MA 02138

5a: Filip Ilievski

5f-1a: Harvard University

5f-c: 12 Oxford Street

Cambridge MA 02138

5a: Lihua Jin

5f-1a: Harvard University

5f-c: 12 Oxford Street

Cambridge MA 02138

5a: Zhigang Suo

5f-1a: Harvard University

5f-c: 12 Oxford Street

Cambridge MA 02138

5a: George M. Whitesides

5f-1a: Harvard University

5f-c: 12 Oxford Street

Cambridge MA 02138

5a: Ramses Martinez

5f-1a: Harvard University

5f-c: 12 Oxford Street

Cambridge MA 02138

5a: Stephen Morin

5f-1a: Harvard University

5f-c: 12 Oxford Street

Cambridge

MA 02138

5a: Robert Shepered

5f-1a: Harvard University

5f-c: 12 Oxford Street

Cambridge

MA 02138

5a: Rui Nunes

5f-1a: Harvard University

5f-c: 12 Oxford Street

Cambridge

MA 02138

## **Scientific Progress**

Please see attached document

## **Technology Transfer**



# BIOINSPIRED, MOBILE ROBOTS WITH HIGH STABILITY, FUNCTIONALITY AND LOW COST

W911NF-11-1-0094

FINAL REPORT  
2/15/11 – 9/30/13

## THE HARVARD TEAM

DARPA/DSO  
ATTN: BAA 10-65  
Dr. Gill Pratt  
3701 North Fairfax Drive  
Arlington VA 22203-1714

Technical POC: Dr. Gill Pratt, DARPA/DSO  
Submission: Gill.pratt@darpa.mil

Submission from:

**George M. Whitesides**  
Department of Chemistry and Chemical Biology  
Harvard University  
Cambridge, MA 02138  
[gwhitesides@gmwgroup.harvard.edu](mailto:gwhitesides@gmwgroup.harvard.edu)  
Tel: 617 495 9430  
Fax: 617 495 9857

**Robert Wood**  
School of Engineering and Applied Sciences  
Harvard University  
Cambridge, MA 02138  
[rjwood@eecs.harvard.edu](mailto:rjwood@eecs.harvard.edu)  
Tel: 617 384 7892

*Laboratory Manager*  
T.J. Martin  
[tjmartin@gmwgroup.harvard.edu](mailto:tjmartin@gmwgroup.harvard.edu)  
Tel: 617 495 9432  
Fax: 617 495 9857

In this final report, we summarize the results of our M3 project. The project evolved from developing and investigating the design rules of PneuNets, to our development of prototypes of soft robots, to new types of actuators, our improved understanding of undulatory locomotion, new assembly methods of soft robots, use of higher strength materials, use of camouflage, to testing of soft robots under harsh conditions.

## 1. PROTOTYPES OF SIMPLE SOFT ROBOTS

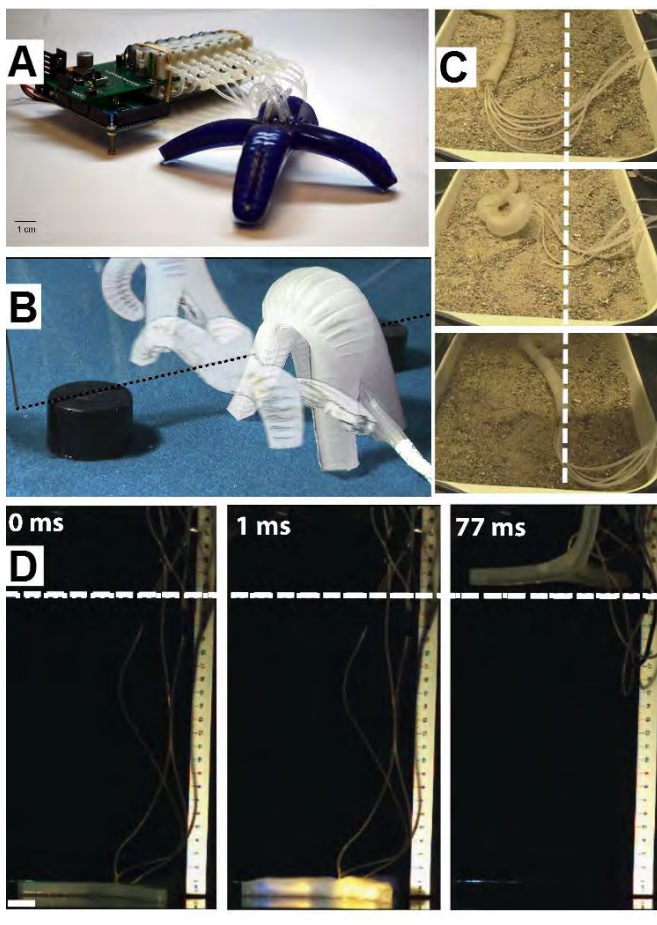


**Figure 1.** **A** Starfish walker that is operated via a battery operated microcompressor array. **B** Quadrupedal robot that can navigate obstacles via crawling and undulating gaits. **C** Snake-like robot capable of being driven in a “sidewinder” like gait. **D** A tripedal robot that can jump.

The microcontroller is also available in a much smaller form factor which allowed us to design an untethered system. The Arduino microcontroller provides the possibility of adding sensors for feedback to control locomotion dependant on some external factor – a wall, or incline perhaps, we also investigated the use of e-GaIn based soft sensors.

We developed at least five different mobile soft robot architectures (Figure 1; not shown is an undulating sheet that we can drive on water and mud). One robot is capable of walking over sandy terrain and moving in any direction without needing to turn (Fig. 1A). Another robot is capable of changing gait from crawling to undulating in order to navigate obstacles or traverse soft – muddy terrain (Fig. 1B).

We also developed a snake-like robot that is capable of moving on sandy terrain (Fig. 1C); however, logically controlling the motion of this robot was difficult. We worked with the Choset group at CMU to develop gait strategies for this type of robot.

We also explored a jumping robot with a tripedal body architecture (Fig. 1D). This robot is powered via the combustion of methane, which rapidly pressurizes the pneumatic networks (pneu-nets) and causes a jumping action. We explored actuation sequences to direct the jumping in different directions.

We developed a pneumatically actuated, quadrupedal soft robot that can **walk** in any of four directions (Figure 2-a). These robots are based on pneumatic networks (pneu-nets), embedded in elastomeric structures, and they contain no hard parts. Each leg of the robot contains two parallel pneu-nets which can be independently actuated. A tether links each pneu-net to a computer controlled compressed air source for actuation. The robot can walk on sand and up a 10 degree incline.

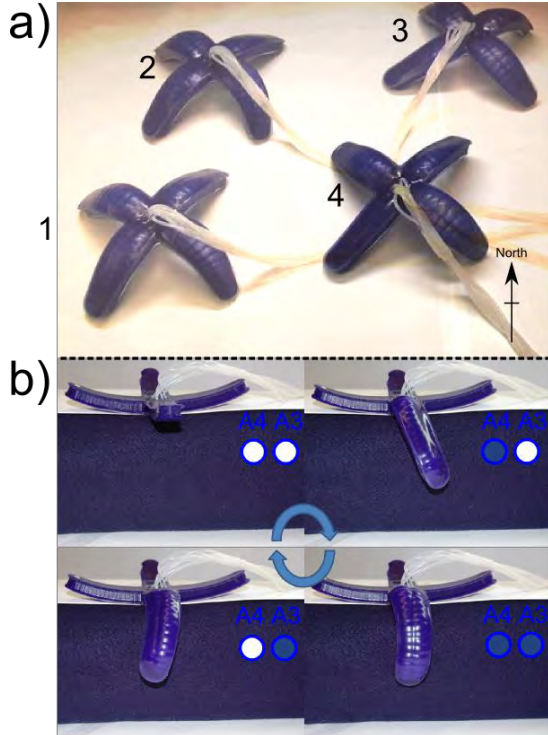


**FIGURE 2.** A) COMPOSITE IMAGE SHOWING THE ROBOT TRAVERSING FLAT TERRAIN. DIRECTIONALITY IS CONTROLLED BY THE SEQUENCE IN WHICH EACH LEG IS ACTUATED. VIDEO OF THE ROBOT WALKING IS AVAILABLE AT [HTTP://YOUTUBE.BE/2IW7E43WOWY](http://YOUTUBE.BE/2IW7E43WOWY). B) A SEQUENCE OF PHOTOGRAPHS DEMONSTRATING THE MOTION OF ONLY THE LEFT HIND LEG OVER ONE CYCLE WHEN THE ROBOT IS PROGRAMMED TO WALK NORTH. TWO PNEUNETS (LABELLED A4 AND A3) ARE ACTUATED IN SEQUENCE (OPEN CIRCLE = NO PRESSURE, FILLED CIRCLE = APPLIED PRESSURE).

## 2. PneuNets

A single PneuNet has one degree of freedom; when pressurized, the PN curls around a single axis (Figure 3). We previously used this capability in a gripping device, to pick up an uncooked chicken egg without damage to the shell.

To retain the design simplicity of PneuNets, while fabricating devices capable of complex motion (several degrees of freedom) we employed a stacking route to device manufacture.

An example of this fabrication route is shown in Figure 4. We stacked three PneuNets (A,B,C) around a central core. This stacked device had three degrees of freedom and, using this device, we swept through an entire hemispherical volume.

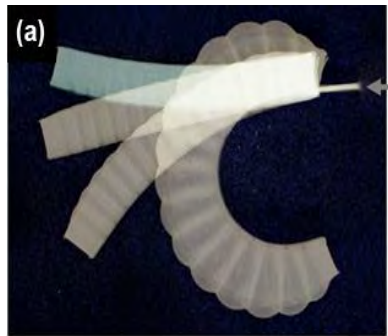


**Figure 3.** Overlay of several snapshots of a PneuNet during its actuation.

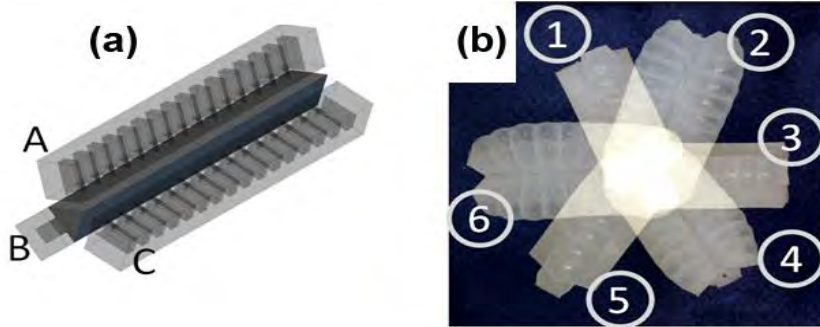


**Figure 4.** (a) Three PneuNets (A,B,C) are arranged around a central core, 120° to one another. The stacked device is capable of three degrees of freedom. (b) Overlaid snapshots of the stacked device during combinations of PneuNet actuation – accessing a hemispherical volume.

### 3. PROTOTYPE ACTUATORS

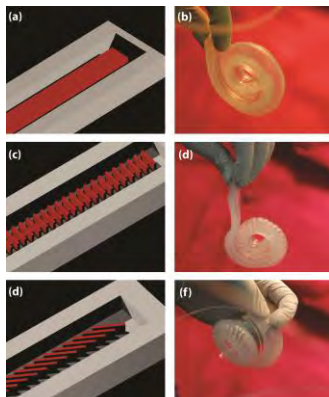


**Figure 5-1.** (left panel) 3D printed molds that define the internal channel geometry of (right panel) soft pneumatic actuators.

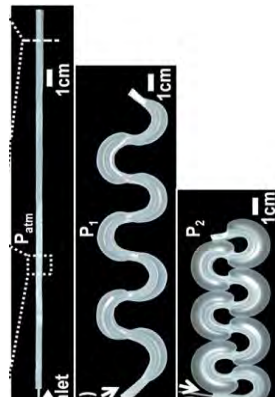


**Figure 5-2.** (left-right) A pneumatic actuator with paper patterned along the length. Upon pressurization, the actuator contracts.

We developed a multitude of “functional modules” hereafter described as actuators. The first functional pneu-net actuators we developed were based on an elastomer inflating and stretching. By bonding the elastomeric channel to an inextensible (“strain-limiting”) layer, the actuator bends when inflated (Figure 5-1). By patterning the interior geometry of the inflating elastomer, we were able to program the actuators to be stiffer (e.g., actuate at greater pressures; Fig. 5-1c,d), or actuate as a helix (Fig. 5-1e,f). We were able to demonstrate that the properties of the pneu-nets are determined by the interior channel geometry; however, the arrangement of the strain limiting layer is also important.

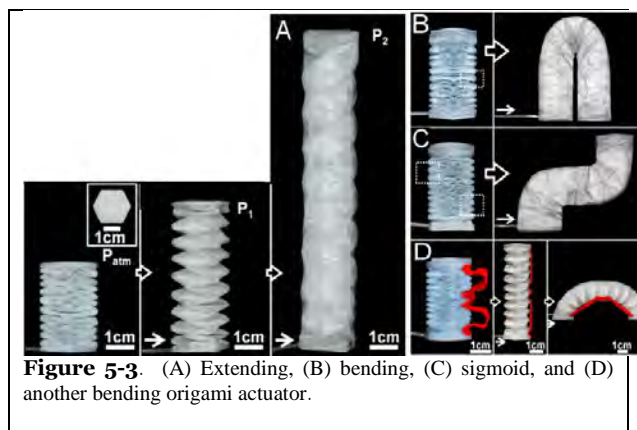


**Figure 5-3.** (A) Extending, (B) bending, (C) sigmoid, and (D) another bending origami actuator.

We increased the sophistication of our actuators through a more complex patterning of the strain limiting layer. An example of one of these actuators is shown in Figure 5-2; the pneumatic network contracts when pressurized, similar in function to a McKibben actuator. Additionally, we used the concept of paper folding (origami) to create paper actuators with complex actuating modes (e.g., extending and multiple bending modes; Figure 5-3).

## 4. PLEATED ACTUATORS

Our soft robot designs relied on highly extensible elastomers for actuation. The PneuNets are pressurized and stretch – by prescribing how they stretch, we fabricated many successful soft-robotic devices. A limitation of these elastomeric PneuNets, however, is their susceptibility to puncture under very large strains (~650%). To reduce sensitivity to puncture and increase our material options for soft-robots, we explored using pleats as a route to large extensibility (e.g., accordion bellows), even in materials that have low strains to failure (e.g., cellulose, Kevlar<sup>TM</sup>, polystyrene).

We designed a two part mold (Figure 6-a) to pattern the exterior and interior pleating and then injected a mixture of the pleating material (chopped Kevlar<sup>TM</sup>) and binder (Ecoflex<sup>TM</sup>). After curing (Figure 6-c), we sealed the pleated actuator to a strain limiting layer (Figure 6-d).

To achieve large amplitudes of actuation using low-strain to failure materials (e.g., elastomers/fiber composites, and fiber mat materials), we fabricated pleated actuators. Figure 7 demonstrates the capabilities of the pleated actuator. Upon pneumatic pressurization, the actuator bends in positive curvature (Figure 7a,b), similarly to elastomeric pneu-nets. When the actuator is placed under vacuum, the actuator bends in negative curvature. (Figure 7-c).

Pleated actuators, thus, increase the material choices available for soft robots and are capable of moving in two directions without the need for antagonistic combinations of multiple actuators. Additionally, these actuators are resistant to puncture due to the stiff fiber matrix and – even after puncture – these actuators seal around the hole (Fig. 8).

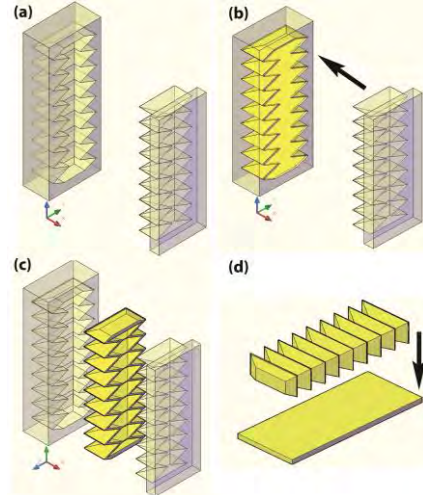


**Figure 6.** (a) Two part mold for soft lithography of pleated actuators. (b) Kevlar<sup>TM</sup>/Ecoflex<sup>TM</sup> (yellow) pressed into mold and (c) replicated Kevlar<sup>TM</sup>/Ecoflex<sup>TM</sup> (yellow) pleated actuator and (d) sealing of the actuator against a Kevlar<sup>TM</sup>/Ecoflex<sup>TM</sup> flat. [arrows indicate direction in which the (b) mold or (d) bellow is applied]

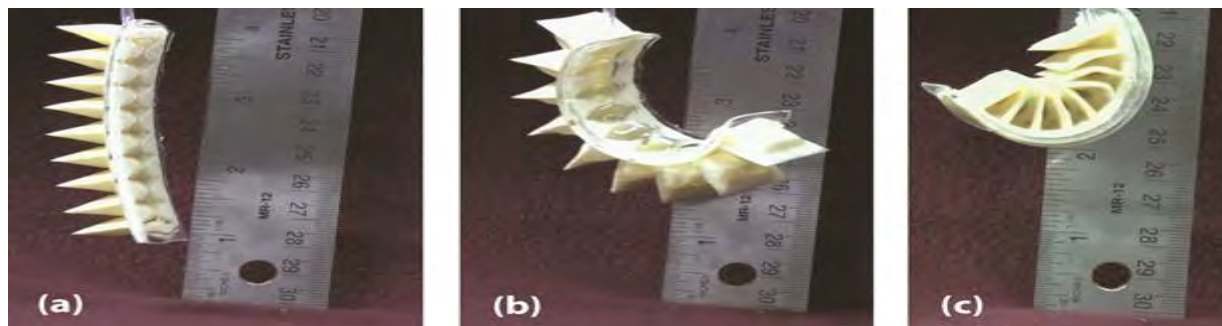


**Figure 7.** KevlarTM/EcoflexTM bellow actuator with internal pneumatic network at (a) ambient pressure, (b) positive pressure (~15psi), and (c) vacuum.

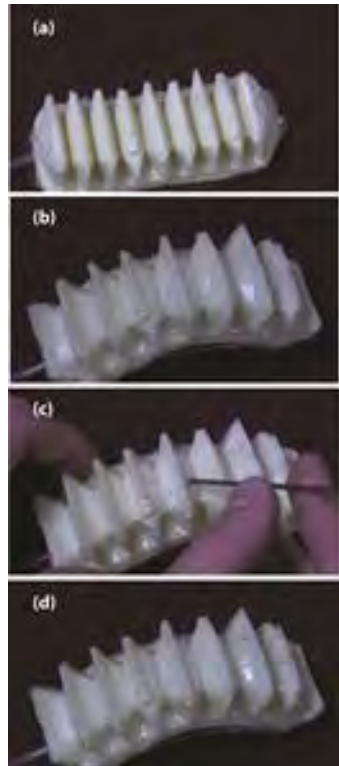


**Figure 8.** (top – bottom), pleated actuator under positive pressure (~10 psi) then stabbed with a 15 gauge needle and then the needle is removed and the actuator still functions.

## 5. IMPROVED PNEU-NET ACTUATORS

Our pneu-net actuators consisted of an extensible top layer and an inextensible bottom layer, and will be referred to as a single-molded pneu-net (sPN) (Fig. 9A). The extensible layer contained chambers connected by a single channel that, when pressurized, preferentially expand the top and inside wall of the chambers, resulting in the bending of the entire actuator due to the compliance mismatch with the inextensible layer. The expansion of the top wall of the chamber is a behavior known as a snap-through instability of the elastomeric material, that is, a dramatic expansion of the elastomeric material to reduce the stress within the system; the inner walls of the chambers also experience strain as the **chambers expand, but they do so within the material's elastic range**. The expansion of both the top and inside walls increases the total amount of compressed gas needed to be transported into the actuator during pressurization; this fundamentally prolongs the pressurization period for these actuators (i.e., slows down actuation speeds).

To determine the amount of mass transport occurring in the actuators, we generated pressure-volume (PV) hysteresis curves and correlated bending motion by continuously monitoring the actuators movement (Fig. 9AB). The actuators were filled with an incompressible fluid (i.e. water) and hydraulically actuated so that a known volume could be measured using the displacement of a programmable syringe pump (Harvard Apparatus PHD 2000). A pressure transducer, connected directly between the actuator and the syringe pump, continuously monitored the pressure inside the system. We pressurized the actuators at a flow rate (0.07614 ml/s) slow enough to avoid dynamic pressure effects (i.e., quasi-static behavior) to simplify analysis. Each cycle consisted of pressurizing the actuator to its fully bent position and then depressurizing the actuator to return to its original position.

There were six important performance parameters that could be extracted from the generated PV plots: i) pressure required for full actuation, ii) volume required for full actuation, iii) input energy required for full actuation, iv) recovered energy obtained from depressurization, v) energy lost during one cycle of actuation, and vi) shape of the PV curve. The maximum values for the x- and y-axis signify the pressure and volume required for full bending of the actuator. The area below the inflation curve during pressurization signifies the input energy of the actuator. Likewise, the area below the deflation curve during depressurization signifies the energy recovered from the actuator. The energy lost is simply the difference between the input and recovered energy.

To compare the sPN and dPN design, we tested actuators made from Ecoflex 30 (for the extensible layer) and PDMS (for the inextensible layer) so that the sPN actuator would fully bend within the range of our pressure sensors. The results show the sPN actuator requires ~3X the pressure, ~8X the volume, and ~35X more energy to fully bend as compared to the dPN actuator. Upon depressurization, the sPN actuator lost nearly 30x more energy than the dPN actuator. In addition, the shape of the dPN actuator is much more linear compared to that of the sPN actuator. The shape of the PV curve of the sPN actuator suggest a snap-through instability behavior that is similar to results obtained in a rubber balloon inflation experiment. The difference in PV shape is important for control since designers prefer linearly responding actuators; the dPN actuator, therefore, has the advantage of providing complex non-linear movement with simple near-linear pressure dependence.

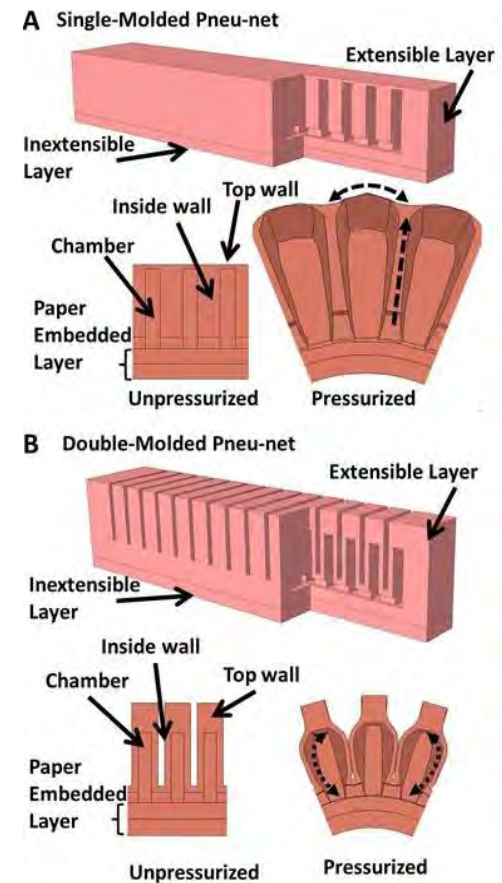


**Figure 9.** Double Molded Pneu-net. A-B) Schematic of the sPN (A) and dPN (B) actuator that consist of an extensible top layer and inextensible paper-embedded bottom layer. The top layer contain of the sPN actuator contains features molded only inside the actuator. The dPN actuator contains features molded both inside and outside the actuator. Solid arrays identify regions of the actuators and dashed arrows signify expanding regions when actuator is pressurized.

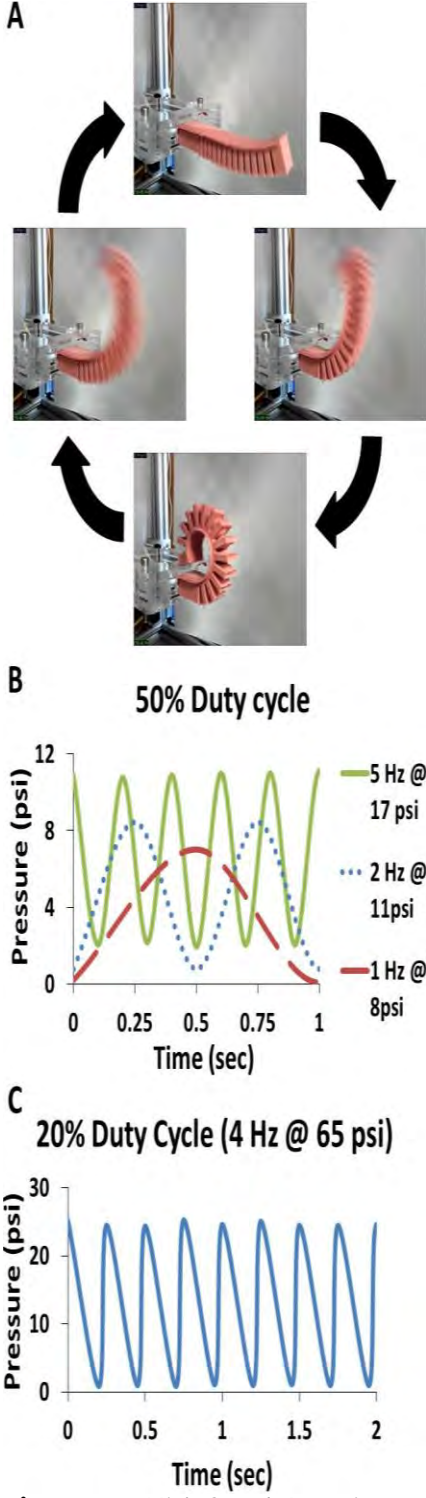


**Figure 10.** High-Speed Actuation.  
A) Images of different positions of the dPN actuator during a full actuation cycle. B) Pressure profile for three symmetric waveform frequencies at pressures that cause the actuator to fully bend.

An important performance criterion for elastomeric actuators is life-span, which is dependent on the fatigue of the material. We consider the life span of an actuator to be the number of full actuation cycles (each cycle consisting of nearly full bending and relaxing) before bursting. The sPN actuator has a life span of ~46 cycles when actuated at 0.33 Hz. The failure of the sPN actuator is due to two reasons: i) the sPN actuator undergoes significant strain causing fatigue of the elastic material, and ii) the sPN actuator is prone to defects (i.e., bubbles) in the top region of the extensible layer. The dPN actuator, however, is not prone to the same defects since the top region of the extensible layer does not undergo any significant strain. This fact, combined with the minimal strain of the material required for bending, enables the dPN actuator to have a life span that we have yet been able to determine. Therefore, instead of life span, we investigated the fatigue experienced by the dPN actuator after cyclic actuation at 2Hz for 10 thousand, 200 thousand, and 1 million actuations. We assessed fatigue by generating PV curves for three separate dPN actuators before and after subjecting them to the cyclic testing. We found that the PV curves do not change substantially but do slightly decrease in slope, meaning that the actuator requires slightly less pressure and more volume to fully bend; this change in slope is a consequence of the elastomeric material softening due to the cyclic loading.

The speed of the dPN actuator depends on the rate of transfer of pressurized gas molecules into and out of the actuator. To achieve rapid bending, we used a computer-controlled solenoid valve to pulse highly pressurized gas for short durations and then vented the system to passively equilibrate with atmospheric pressure (Fig. 10A); the head pressure (pressure set by the regulator) was adjusted to achieve full bending of the dPN actuator. The highest frequency of full bending and relaxing of the dPN actuator achieved using a 50% duty cycle (equal durations of pressurizing and venting periods) was 2 Hz using 11 psi head pressure (Fig. 10B). Higher frequencies did not allow the actuator to return to its original position. We employed a duty cycle with a shorter pressurization period (50 ms using 65 psi head pressure) and a longer venting period (200ms) to achieve an overall higher frequency (4Hz) of actuation (Fig. 10C).

We developed a pneu-net actuator that allows rapid actuation and extended life span that we believe will enable the development of more sophisticated and reliable soft robots. Rapid actuation is beneficial to many soft robotic applications, such as faster movement of mobile robots and quicker manipulation of grippers. The bi-modal behavior that occurs at high speeds could potentially provide sophisticated control schemes to designers. In addition, the more linear dependence between pressure and bending together with the smaller volumetric expansion makes this soft actuator much more appealing for surgical applications that require positioning of tools at precise locations and in tight spaces.

## 6. Rapidly Actuating Pneumatic Networks for Soft Robotics

We developed soft robotic actuators that comprise mm-scale channels embedded in composite elastomers. These structures generate complex motions, but those so far described have been relatively slow (on the order of seconds). Rates of actuation are limited by the large changes in internal volume required in order to achieve their full range of motion. The Pneu Nets also typically fail (e.g. mechanically burst) when higher pressures/flow rates are attempted to achieve faster actuation. We designed Pneu Nets that actuate much more rapidly (<100ms), because relatively small strain is required for full actuation. The new design uses patterned features on both the interior and exterior side of the actuator so that the exterior of the elastomeric material requires minimal expansion upon reaching its full range of motion.

To demonstrate the precision and speed of these fast actuators, we used four of them to play "Mary Had a Little Lamb" on a keyboard (Fig 11A). The four actuators are fixed to a keyboard using Velcro and actuated with 15 PSI controlled by computer-regulated solenoid valves. Each note was played by pressurizing one of the actuators for 75ms and then venting for 150 ms. Each individual note played is shown in the spectrum analysis of the audio file (Fig 11B). We demonstrated that the notes played by the actuators match those of the song and are clearly resolved. The system plays the entire two staves within 6 seconds, and three notes in as little as 0.4 seconds.

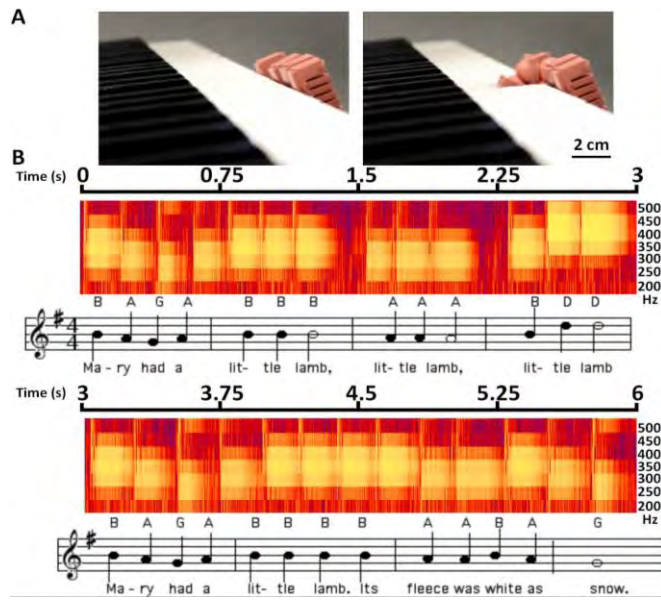


**Figure 11.** Independent Output Control. A) Images from two views of four fPN actuators playing a tune on a digital keyboard. Each fPN was actuated for 75 ms at 103 kPa (except for repeated notes, which were actuated for 50 ms) and vented for 150 ms. B) Spectrum analysis of the audio file for frequencies between 200 and 500 Hz.

## 7. FIBER REINFORCED ACTUATORS

In 2013 we made several advances in the development of fiber reinforced soft actuators and their application in robotic systems. In soft actuator development, we have developed a method to mechanically program on-the-fly an actuators bending radius and location. We also developed a fiber reinforced multi-degree of freedom bending actuator. We integrated these actuators into a versatile manipulator and mocked up a hexapedal locomotion platform.

### A. Mechanically Programmable Bend Radius for Fiber-Reinforced Soft Actuators

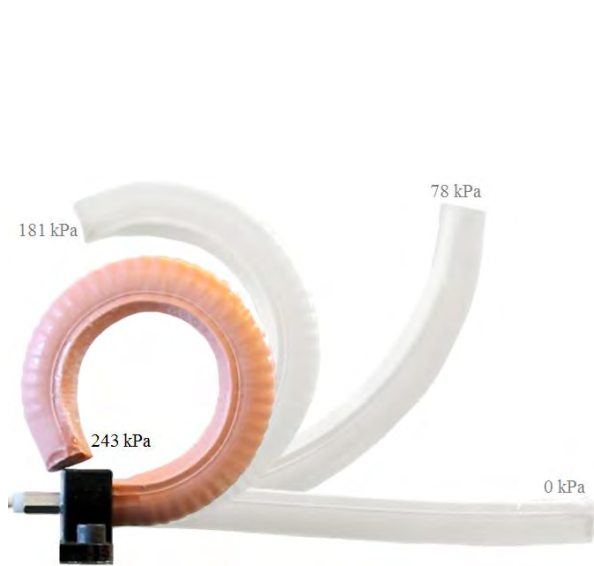


**Figure 12.** Range of motion of the fiber reinforced soft bending actuator constructed from 28A durometer rubber (see Table I for material properties).

We developed a method to alter the motion of a soft bending actuator on-the-fly. This is achieved with a form fitting covering - a sleeve - that acts as a strain limiting layer in all directions and significantly restricts covered portions from bending (Fig. 12). The sections of the actuator that are not covered are free to bend. Adjusting the amount of free area between two sleeves impacts the location and the magnitude of the actuator's bending radius of curvature. In practice, this is demonstrated in Fig. 13 with three different sleeve spacings: 0 (a single cut), 15 and 30 mm centered at the actuators midpoint.

The sleeve material chosen for this work is Sure-Grip heat-shrink tubing, which is a polyolefin/polyester woven fabric that shrinks when heat is applied. Heat shrink tubing has many desirable properties including the ability to conform around irregular shapes, rapid installation (< 1 minute), simple alteration (i.e. cut to length or cut holes to create free space), and reversibility as it can be removed with cutting tools. The sleeves also offer a unique capability for interfacing rigid elements with a soft actuator. From a mechanical perspective, incorporating passive rigid elements into a soft actuator assembly has the advantages of constraining radial expansion on the flat surface and further stiffening actuator sections where bending is not desired. Fig. 14 illustrates this concept where Figs. 14a-b, depict the bowing of the actuator's flat surface during pressurization with an illustrated cross section and actual side view. When FR laminate sheets (0.8 mm thick fiberglass laminate) are added and covered with a sleeve (Figs. 14c-d), the sleeve anchors the fiberglass paddles, and the fiberglass paddles further reinforce the sleeved areas from bending (Fig. 15).

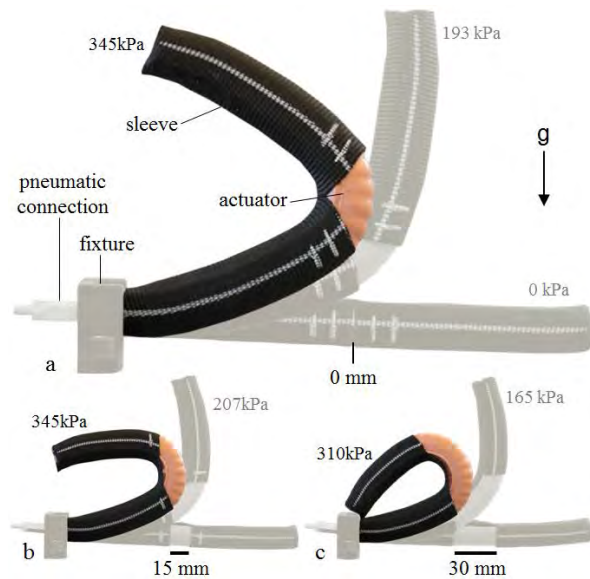


**Figure 13.** Range of motion comparison of a 28A durometer sleeved soft bending actuator at different sleeve spacings with (a) 0 mm, (b) 15 mm, and (c) 30 mm sleeve spacing. The shadow images show the actuators bending at different pressures.

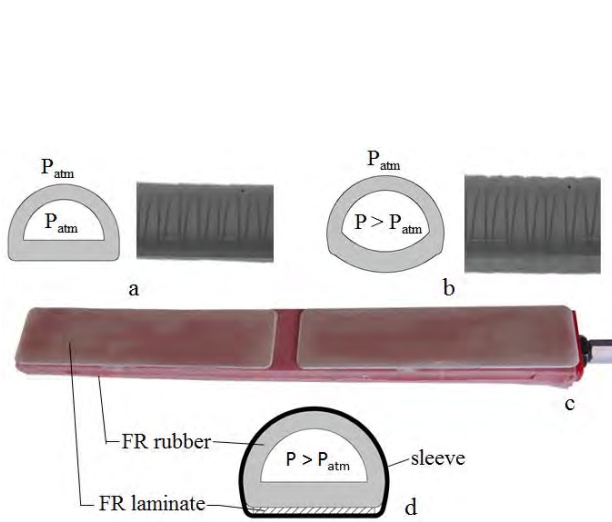


**Figure 14.** Illustrated cross-section comparison of fiber reinforce actuator with and without fiber reinforced laminate where (a) shows an illustrated cross-section and actual side view of an unpressurized FR actuator, (b) shows expansion of the actuator walls due to fluid pressurization (note the outward bowing of flat face), (c) demonstrates placement of FR laminate on a FR actuator, and (d) shows an illustrated cross-section view of the actuator when a sleeve is added. The combination of the sleeve and FR laminate stiffen the flat face and eliminate visual indications of bowing.

As part of an empirical evaluation, three actuators were created; one with 10A and another with 28A durometer silicone rubber. The third actuator, also constructed of 28A, encloses all FR laminate in the sleeved portions as depicted in Fig. 2.4 and will be referenced as 28A-FRL. All three actuators were tested at the three sleeve configurations: 0 mm (a single cut), 15 mm, 30 mm spacing. Each actuator was cantilevered in an evaluation platform with one end - the pneumatic connection - anchored to a fixture (see Figs. 12 and 13). The unsupported actuator length was 16 cm (6.3 inches) for all cases. The 10A durometer actuator was pressurized up to 207 kPa (30 psi) while the 28A durometer actuators were pressurized up to 414 kPa (60 psi).

During these experiments, a camera captured frames for post-analysis of the bending angle and radius. The results of the soft actuator experiments reveal tradeoffs in actuator performance between the sensitivity of angular deflection to fluid pressurization, output force, and radius of curvature. With respect to angular deflection, the lower durometer rubber (10A) demonstrated the highest sensitivity to pressurization (see Fig. 16 and Table 1 for slope values). Sleeve spacing also affected sensitivity, where increased spacing correlated to increased deflection at a given pressure. This pattern appeared across all tested actuator types. As shown in Table 1, the slope from 0 mm to 30 mm configurations more than doubled for the 10A and 28A-FRL actuators, and increased 1.6x for the 28A actuator.

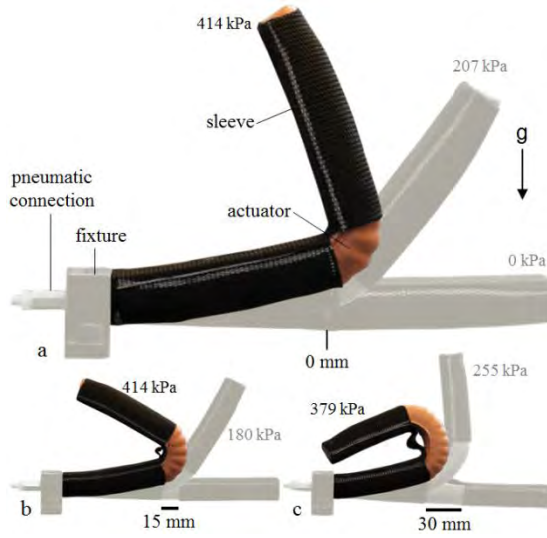


**Figure 15.** Range of motion comparison of a 28A durometer sleeved soft bending actuator at different sleeve spacings with (a) 0 mm, (b) 15 mm, and (c) 30 mm sleeve spacing. The shadow images show the actuators bending at different pressures.

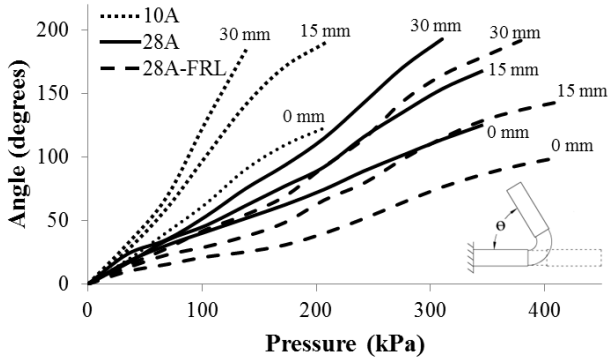


**Figure 16.** Deflection angle between the two sleeved portions of the 10A, 28A, 28A-FRL actuators for a range of input pressures.

With respect to tip force measured from the neutral position, the higher durometer rubber was able to support higher pressures and thus produce larger output forces (Fig. 17). For example, all sleeve configurations for the 28A-FRL actuator exceeded 5 N with the 30 mm configuration delivering the largest distal force of 7.12 N at 414 kPa (60 psi). In the 10A configuration, the 30 mm sleeve spacing produced the highest output force of 2.75 N at 172 kPa (25psi), and decreased marginally with the smaller sleeve spacings. It may be the case that the larger sleeve spacing correlates to a more active actuator area and can contribute marginally more force. When the end-point forces of all three actuators are evaluated together, they follow a similar trajectory (Fig. 17). The commonality among all three actuator configurations are the fiber reinforcements (i.e. woven fiberglass strain limiting layer and Kevlar thread winding) embedded in the actuator body. The close packing of the curves suggests that the fiber reinforcements play a larger role in the output force response of these actuators than material durometer (at least at low pressures). At high pressures, the 10A durometer actuator is unstable and prone to failure (e.g. they will easily fail at 400 kPa). Our experience suggests that while a lower durometer rubber may initially produce forces similar to a higher durometer rubber, the higher durometer rubber can support higher pressures and produce larger forces. This is a topic that deserves further investigation evaluating multiple FR configurations.

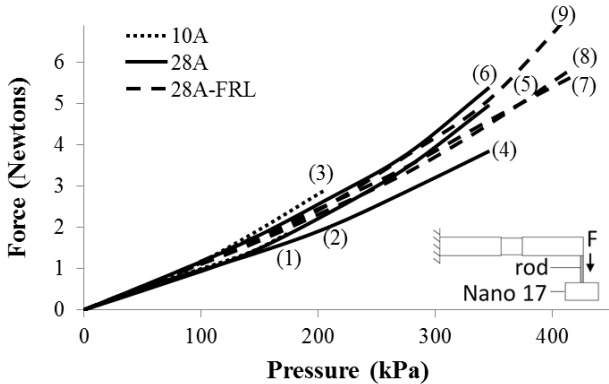


**Figure 17.** Force results for all actuator configurations. There is a similar output force response for these three different actuators. The only commonality between the actuators is the fiber reinforcements. The number next to each curve corresponds to the ‘Actuator Type Identifier’ in Table I.

The radius of curvature measured at the maximum evaluated pressure increased as sleeve spacing increased (Fig. 18). Between the 10A and 28A durometer actuators, the 10A actuator is able to achieve a

ACTUATOR PERFORMANCE & LINEARITY				
Actuator Type Identifier	Actuator Type	Sleeve Cut Size	Slope ( $\Delta y/\Delta x$ )	$R^2$
1	10A	0 mm	4.24	0.9948
2	10A	15 mm	6.59	0.9913
3	10A	30 mm	8.57	0.9743
4	28A	0 mm	2.53	0.9957
5	28A	15 mm	3.3	0.9953
6	28A	30 mm	4.07	0.9889
7	28A-FRL	0 mm	1.61	0.9762
8	28A-FRL	15 mm	2.4	0.9885
9	28A-FRL	30 mm	3.41	0.9808

**Table 1.** Specifies the slopes of the curves in Fig. 5, where a larger slope values means the actuators deflect more with less pressures. The  $R^2$  column confirms a linear response between input pressure and angle of deflection of the test pressure ranges.

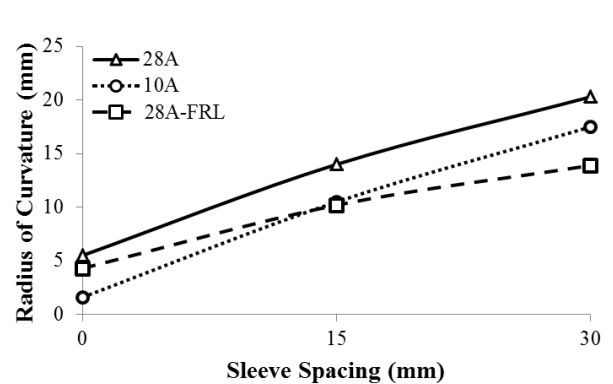


**Figure 18.** Measured radius of curvature at maximum evaluated pressure.

smaller radius of curvature for all sleeve spacing configurations. The 28A-FRL actuator showed the flattest response. At the zero mm sleeve position, the 28-FRL radius of curvature falls between the 10A and 28A; however, by the 30 mm sleeve spacing, this configuration achieved the lowest radius of curvature. This suggests that the FR laminates localize actuation to the sleeve spacing. Therefore, to achieve the tightest radius of curvature with a higher durometer rubber, a passive stiffening element such as FR laminate should be included.

The value of this innovation is apparent in the following case study which evaluates the ability of two opposed 28A durometer actuators (Fig. 19) to shape match an angular object and the resulting payload holding capacity. The object is a rigid foam block (11 cm x 13 cm x 2.5 cm) and has a metal hook passing through which connects to a hanging bucket. The actuators were pressurized to 345 kPa (50 psi) and sand was gradually added to the bucket until the object dropped. Three actuator cases were tested including the standard sleeveless bending actuator, the zero mm sleeve spacing, and the FR laminate zero mm sleeve configuration. To minimize material friction comparisons, a small amount of sleeve material was bonded to the flat face of the rubber bending actuator to match the surface properties of the other cases.

The standard bending actuator (Fig. 19a) bows at the sides leaving considerable compliance for the actuators to deform with increasing payload. The zero mm sleeve configuration (Fig. 19b) bows much less at the sides and demonstrates improved conformability. The FR laminate and sleeve configuration demonstrates the best conformability (Fig. 19c). In this preliminary study, the average payload capacity of the respective configurations is 3.45 kg, 4.68 kg, and 6.1 kg. This suggests that the proposed soft actuator sleeve method can be used to limit compliance of covered portions and increase payload holding capacity.

For the purpose of demonstration, Fig. 20 highlights the ability to rapidly alter the motion of a bending actuator by modifying the sleeve on-the-fly. In this example, a bending actuator was outfitted with three FR laminate segments. Fig. 20a shows the pressurized state without any spacings cut into the sleeve. Fig. 20b shows the same actuator with a single cut in the sleeve near the distal end. Fig. 20c shows the simplicity of adding a second joint and Fig. 20d demonstrates that sleeved portions can be cut away to recover bending motions. Figs. 20e-f further illustrate that the sleeve can be used to move the point where the actuator initially bends.

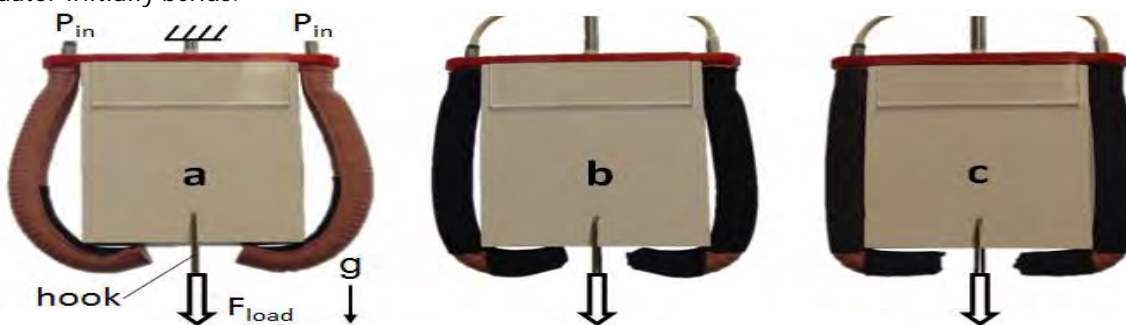


**Figure 19.** The proposed sleeve method enables improved shape matching to angular objects and holding strength.

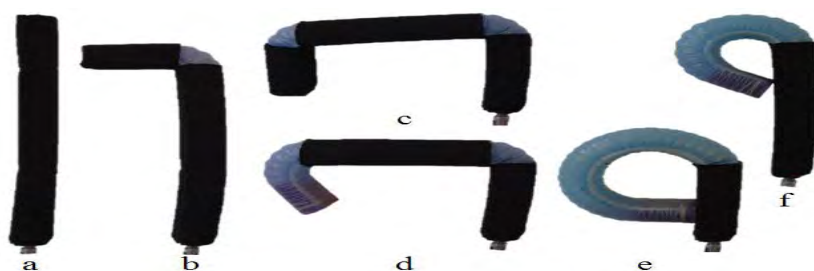


**Figure 20.** The sleeve applied to a bending actuator to generate a range of motions.

## B. Fiber reinforced Multi-DOF Bending Actuator

In early 2013, we developed a process to fabricate multi-DOF fiber reinforced soft actuators, which built on our work from 2012. Three fiber reinforced linear soft actuators were co-molded together into a single body (Fig. 21). Activation of one chamber causes the structure to bend in one direction (Fig. 22). Activation of two or more chambers enables 2-DOF motions. In this arrangement, the fiber reinforcements prevent one chamber from swelling into and affecting its neighbors. There is also an opportunity to incorporate a working channel as shown in Fig. 27.



**Figure 21.** Multi-DOF bending actuator consisting of three fiber reinforced linear actuators co-molded together.



**Figure 22.** Gradual pressurization of one of three chambers.

### C. Soft Actuated End Effector

The i-HY (Fig. 23) hand was developed under DARPA's Autonomous Robotic Manipulation - Hardware Track (ARM-H) program with the goal of creating durable, inexpensive robotic hands capable of manipulation as well as grasping, suitable for use on mobile robots (note this was developed in a collaboration between Harvard, Yale, and iRobot). This cable driven, under actuated hand is capable of performing a wide range of grasping and in-hand manipulation tasks using 5 servo motors.

We used this hand design as inspiration for a soft robotic version (Fig. 24) in which 1 servo motor rotates two fingers (Fig. 25) to expand the grasping range and a compressed air source actuates the fingers. Some notable features of this design include

- Simple finger replacement – after disconnecting the pneumatic line a finger can be threaded on or off and replaced with a smaller or longer finger.
- No cables – eliminates design challenges of cable path and cable wear.
- Robust construction – there are no moving parts in the rubber fingers.
- Safe human-robot interaction – the pressurized finger are back drivable.
- Adaptable Morphology – fingers conform to irregular objects and distribute pressure.
- Parallel actuation – a single compressed air source can be used to actuate many digits.



• **Figure 23.** i-HY Hand



**Figure 24.** Soft Actuated version of i-HY Hand

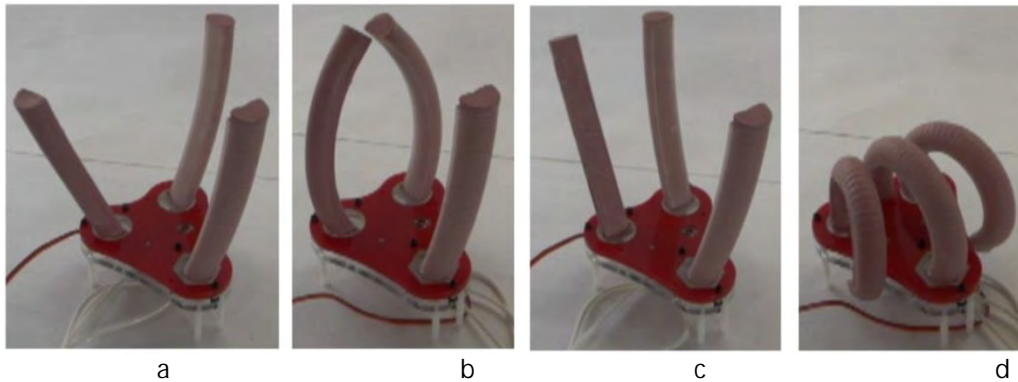


**Figure 25.** a) One pose where two fingers face each other and b) are pressurized to connect. c) The two fingers rotate 90 degrees and d) all fingers are pressurized to perform a power grasp.



**Figure 26.** All fingers are activated to conform around and pick up a quart sized metal can.

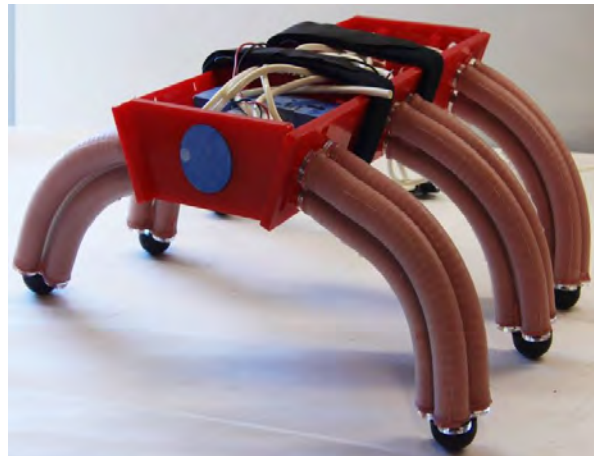


**Figure 27.** Mockup of a hexapedal locomotion platform using the multi-DOF soft bending actuators as legs.

## 8. TRANSPARENT REEL-TO-REEL ACTUATORS

We reported, in Q3 of 2012, our efforts aimed at developing ultra-low cost, robotic actuators. We focused on commodity materials (e.g., polyethylene films, tape, and paper) and lamination-style fabrication that is compatible with reel-to-reel processing. This approach extends the library of material that can be used to fabricate robotic actuators and presents the opportunity to fabricate robotic elements on a large scale. In addition to these practical advantages, the actuators we are creating are extremely lightweight and thin, opening the door to new applications (e.g., active airfoils). The methods and materials we are using to fabricate these actuators place them in the same class of consumables as trash bags and newspapers.

Progress yielded ultra-thin and *transparent* pneumatic actuators (Fig. 28). This development is significant because the actuators are virtually undetectable by eye meaning they can operate in front of things you may want to see (e.g., a television screen) without obstructing the view and they can blend in nearly anywhere. We continue to work on how to incorporate reflective elements and optical gratings to add functionality that take advantage of the transparency of these actuators.

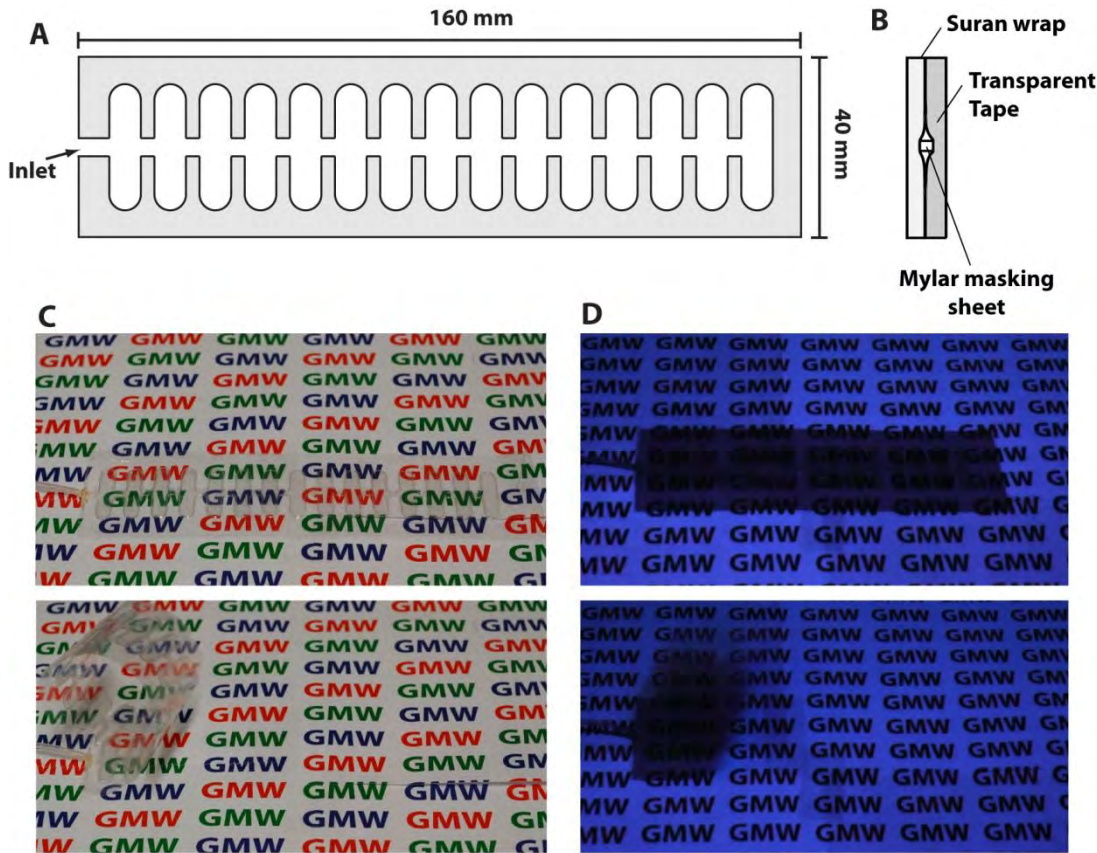


**Figure 28.** Ultra-thin, transparent actuators. A) Dimensions of the actuator shown in C and D. B) Cross-section of the actuator showing the laminated materials. C) Photograph of the actuator at rest (top) and when it is actuated (bottom) by pressurizing the pneumatic channels through the air inlet shown in A. D) When illuminated with ultraviolet light the location of the actuator from C is apparent.

## 9. ROLL UP FABRICATION OF ACTUATOR MODULES

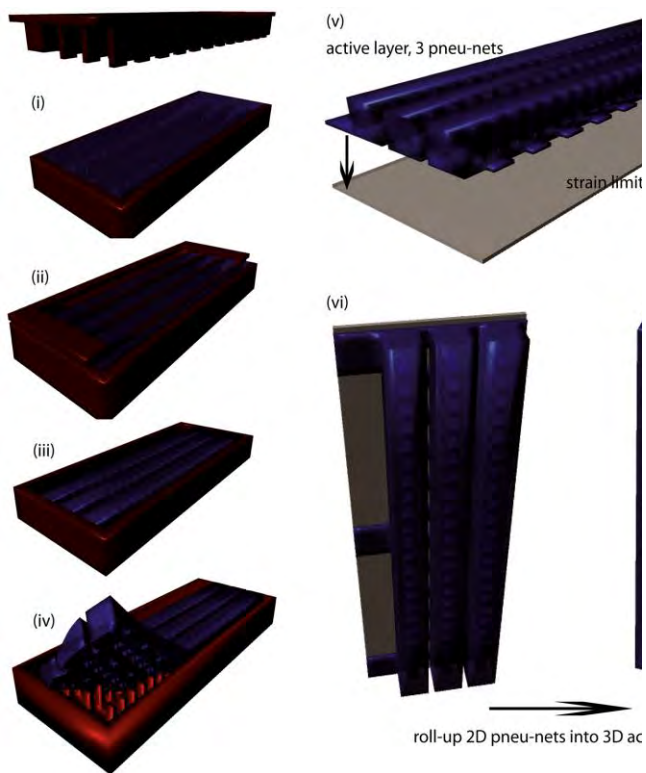


**Figure 29.** (i-iv) 2 part mold and soft lithography method to form an actuator with three parallel pneu-net channels. (v) Bonding of the pneu-nets to the strain limiting layer and then (vi) rolling up of the 2D pneu-nets into a three DOF actuator.

seven different levels of stiffness can be directly printed actuators that can withstand thousands of actuations by minimizing delamination between hard and soft interfaces by printing discrete gradients of the materials in order to distribute stress of the materials at the expanding junctions (Fig. 30 b). We also built bending actuators and grippers (Fig. 30 c-d) similar to those fabricated using molding procedures with two-part elastomers.

We previously demonstrated a three degree of freedom (DOF), tentacle actuator that is capable of accessing a full hemispherical volume of space. The tentacle actuator is composed of three hollow pneumatic channels arranged, cylindrically, 120° to one another. Using this actuator, we have fabricated versatile manipulators capable of picking up and repositioning a variety of objects. The 3D molding technique used to fabricate this actuator, however, limits the pneumatic channel geometry.

To achieve pneu-net architectures, within a three DOF actuator, we developed a method of using our existing 2D soft lithography method and then rolling the pneu-nets into a three DOF, tentacle actuator (Figure 29). These three DOF modules are capable of accessing the same hemispherical volume as the previous tentacle actuators, however, the increased surface area of the pneumatic network should allow for greater applied force using similar channel pressurization. This capability will be useful for applications requiring greater force, such as manipulating heavy objects and transportation of payloads.

## 10. 3D PRINTED SOFT ROBOTS

We investigated how to use a 3D printer to directly fabricate soft actuators without a molding step (fig. 30 a). Using a Connex objet 3D multi material printer, both soft and hard materials of

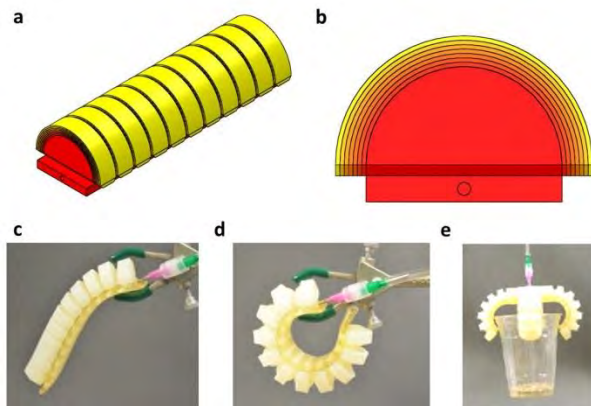


**Figure 30.** a) CAD of a 3D printed actuator with a soft body and hard shell. b) View of the front face of the actuator to visualize the gradient of materials printed between the hard and soft bodies. c-d) Images of the actuator in a unpressurized (c) and pressurized (d) state. e) Image of a 3D printed gripper lifting a 50g cup of sand.

## 11. SCALABLE FABRICATION OF ROBOTS: 7 CM TO 1 METER ROBOTS

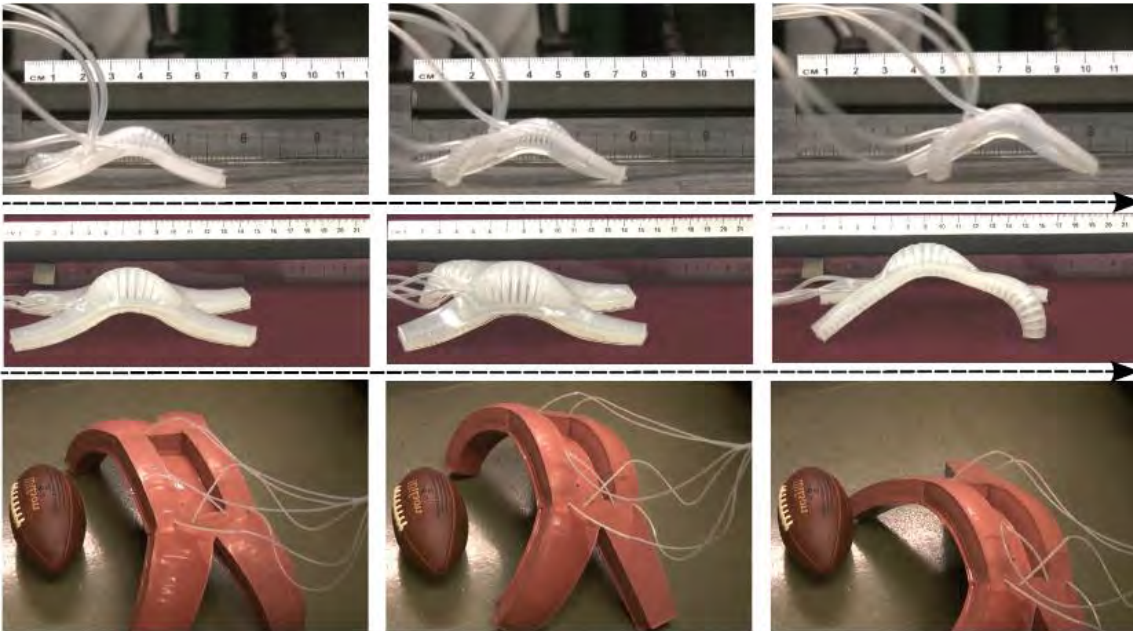


**Figure 31.** (Top) Small (7 cm long) and (Middle) original (15 cm long) quadrupedal, gait changing robots composed of 100 kPa modulus silicone (Ecoflex 0030). These robots are operated at ~7 psi. (Bottom) ~1 Meter long quadrupedal, gait changing robot composed of higher modulus (**1 MPa; M4601™**) silicone elastomer. This robot is operated at ~25 psi. The dashed arrows in each panel indicate the approximate direction of travel from left to right.

Our early results demonstrated that we have several power sources for these soft robots, but few practical methods of using them in untethered operation, at the weight our robots could carry. Soft lithography presents a route to fabricating robots at multiple size scales, without changing the design or method of assembly. To demonstrate the scalable fabrication of soft robots, we molded larger and smaller sizes than the original 15 cm long gait changing robot (Figure 31). The smaller robot (Figure 31, Top) could be useful for navigating through tiny cracks and the larger robot (Figure 31, Bottom) is capable of carrying loads in excess of 25 lbs, sufficient for untethered power sources.

As the length, L, of the robot increases, the surface area increases as  $L^2$ , and this is proportional to the force the pneumatic actuation applies. The weight of the robot increases as  $L^3$ ; there is thus a limit at which the applied force is not sufficient to carry the weight of the robot. In order to carry the weight of the large quadruped (~3 kg), we needed to apply greater pressures – resulting in larger applied forces. The low modulus of the Ecoflex 0030 (~1 kPa; Figure B1-2) we used resulted in rupture of the actuators at pressures in excess of 10 psi; high modulus silicone (~1 MPa; M4601, Wacker Chemical; Figure 32) pneu-nets sustained actuation pressures of > 25 psi.

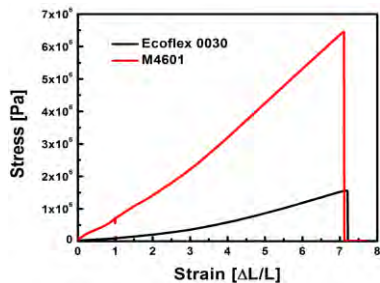


**Figure 32.** Stress vs. strain curve for two different silicone elastomers: (red) M4601 with an Young's modulus of ~1 MPa and (black) Ecoflex 0030 with a Young's modulus of ~100 kPa.

One liter of liquid CO<sub>2</sub> could potentially actuate a small soft robot over 10,000 times, but a 1L container of this material is too heavy for the Ecoflex 0030 based robot to carry. The new, larger quadruped can carry

many of these liquid CO<sub>2</sub> cylinders; however, it requires greater pressures (~20 psi) and more gas volume (~200 ml) for actuation. After recalculating the number of actuations available from 1 L liquid CO<sub>2</sub>, for 20 psi and 200 ml actuations, the new value is ~1,600 actuations. Empirically, for our currently unoptimized gait, one duty cycle of the robot (four leg motions) results in ~.6 M travel distance. Thus, a crude estimate of the distance this quadruped can travel on 1 L of liquid CO<sub>2</sub> is  $1,600 \times 0.6 / 4 = 240$  meters. Since 1 L of liquid CO<sub>2</sub> weighs < 1 kg and the robot can carry >11 kg, then the robot may be able to operate, untethered for up to  $\sim 10 \times (240) \sim 2.5$  km.

## 12. Ultra-low cost robotic actuators

We explored alternative methods and materials for the fabrication of ultra-low cost robotic actuators. Everyday materials such as bubble wrap, saran wrap, and scotch tape, are suited for this approach and have the advantage that they are readily available almost anywhere. Examples of these new actuators are shown in Figure 33. This approach extends the library of material that can be used to fabricate robotic actuators and presents the opportunity to fabricate robotic elements almost anywhere with simple tools (e.g., scissors and rolling pins). In addition to these practical advantages, the actuators we are creating are extremely lightweight and thin, opening the door to new applications (e.g., active airfoils). The methods and materials we are using to fabricate these actuators place them in the same class of consumables as trash bags and newspapers.

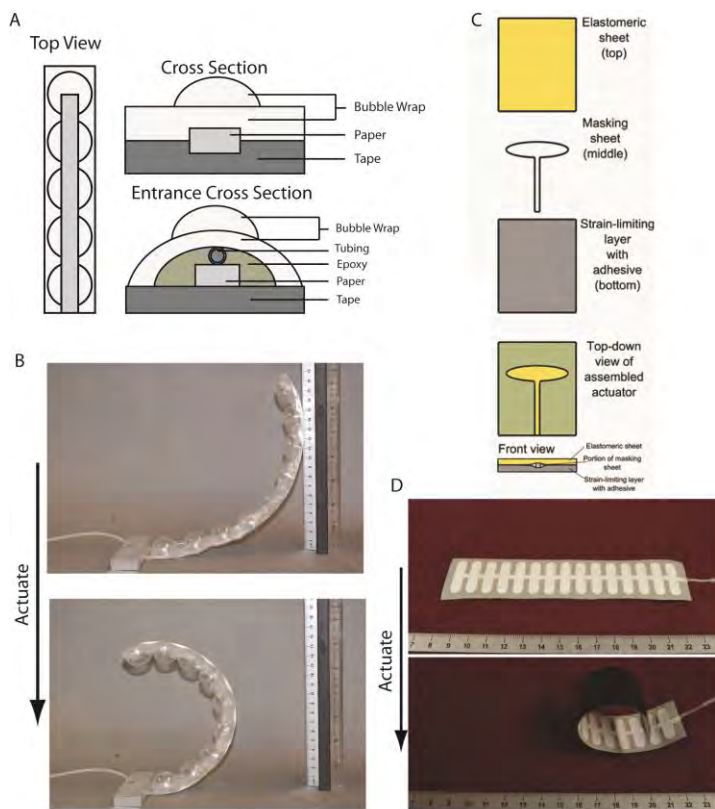


**Figure 33** (A) Schematic of an ultra-low cost actuator fabricated from bubble wrap. (B) Photographs of a bubble wrap actuator bending when pressurization with air. (C) Schematic showing the layers of an ultra-low cost actuator fabricated from saran wrap, paper, and tape. (D) Photographs of a saran wrap/tape actuator with 15 segments curling up when pressurization with air.

## 13. REVERSIBLE, SOFT SEAL ASSEMBLY OF SOFT ROBOTS

The design phase in robot manufacturing is typically long and costly; lego-like assembly of multifunctional modules into robotic systems would allow rapid design iteration, reducing both of these metrics. We used the reversible deformability of elastomers to join modules using soft-seals, allowing rapid assembly of robots from prefabricated modules (Figure 34). Additionally, we attempted to identify the minimum set of modules necessary to fabricate robots able to simulate the function of a unibody design. As a first demonstration, we used this design tool to fabricate a gripper and quadruped robot (Figure 35).

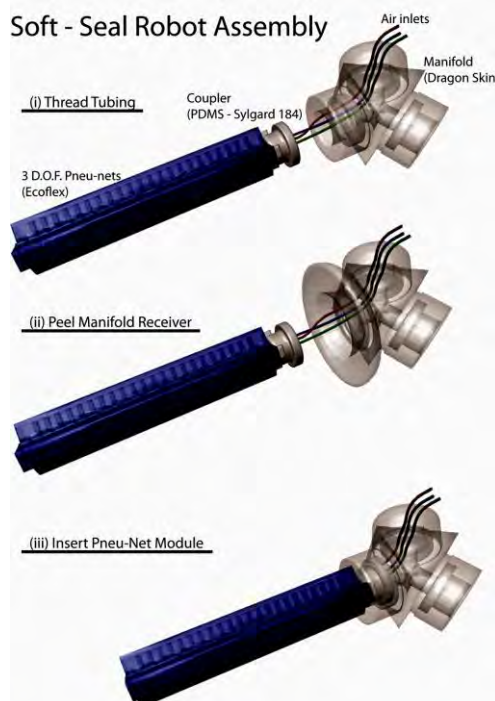


**Figure 34.** (i-iii) 3 DOF actuator module insertion into elastomeric manifold. (ii) The ports in the manifold can be peeled back to reversibly join the modules.



**Figure 35.** (left to right) Three modules assembled into a three port soft manifold to form a gripper – shown picking up a paper cup. Then four modules joined to two manifolds, where the two manifolds are similarly joined together – the final form is that of a quadruped.

## 14. MODULAR ASSEMBLY OF ARBITRARY ROBOT ARCHITECTURES

Soft robots, and robots in general, are not easily reconfigured. The size, type, and arrangement of the pneu-net actuators in soft robots (e.g., grippers and walkers) are fixed by the master—a different master is required to create each robot. The creation of soft robotic modules (e.g., actuators and hubs) that we can easily connect in different configurations, like Lego® blocks, will enable us to construct different robots from a common set of components. Using this approach we can: (i) disassemble the modules used in one robot and reuse them to build a new one, (ii) easily connect one robot to another, (iii) easily modify parts of existing ones, and (iv) repeat any of these operations multiple times.

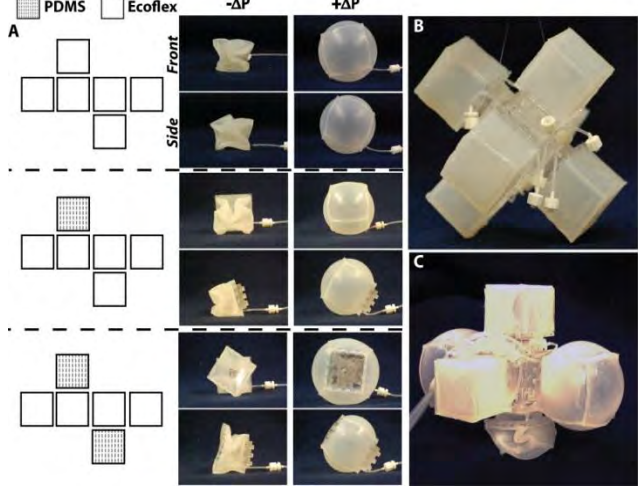


**Figure 36.** Modular assembly of soft robots. (A) Three examples of different cube actuators. The key on the left illustrates the material used for each face. The two columns of images show side and front views of the cubes actuated using negative and positive pressure. (B) Six cube actuators are attached to a central hub creating a soft robot that uses tumbling to locomote. (C) The actuators used to construct the robot in B can be independently controlled. In all examples the cube sides (in an un-actuated state) are 4.5 cm.

void space in the actuator and hub modules by embedding electronics, batteries, and compressors that can run the robot. We also plan to explore the assembly of soft robots using different legs, tentacles, and other pneu-net actuators following a similar strategy.

## 15. MAGNETIC ASSEMBLY OF SOFT ROBOTS

The functions and capabilities of earlier examples of robots were constrained by the connectivity of modules that were pre-assembled manually. Although using pneumatically triggered disassembly allows subtractive modification of these robots, a complementary method for remote assembly will significantly expand the number of options available to a teleoperator in adjusting the functions of robots according to the situation.

To test the combination of pneumatic actuators and magnetic connectors for remote assembly of a robot, we equipped a hybrid quadruped with two hard containers, each magnetically coupled to an inflatable connector (**Fig. 37 a**). This robot, which we called a “porter,” was equipped with a left container for carrying a magnet-embedded soft gripper, and a right container that held two spheres to balance the weight of the gripper. A modified soft tentacle with a ring magnet at the apex and a poly(ethylene) tube through the central channel was assembled at the center of the porter.

We directed the robot to walk towards its target (a green sphere) using pneumatic actuation (**Fig. 37 a**). Inflating the side channel on the right (**Fig. 37 b**) of the soft tentacle pneumatically caused the soft tentacle to bend towards the left container carrying the soft gripper. Attractive magnetic force between the gripper and the magnet at the apex of the bent tentacle pulled the two soft units together at close range, and **self-aligned** the central, open pneumatic channel of the soft tentacle with that of the soft gripper.

To test the function of the remotely assembled soft tentacle-gripper in manipulating centimeter-sized object, we used the tentacle to position the gripper above the target (**Fig. 37 c**), actuated the gripper to pick up the sphere (**Fig. 37 d**), re-positioned the gripper with the tentacle using pneumatic control, and released the object into the empty container on the left (**Fig. 37 a**). After the robot moved forward over a short distance, we remotely disconnected the magnetically attached containers from the quadruped by inflating the integrated bladders, and thus completed the delivery of its cargo (**Fig. 37 h-j**).

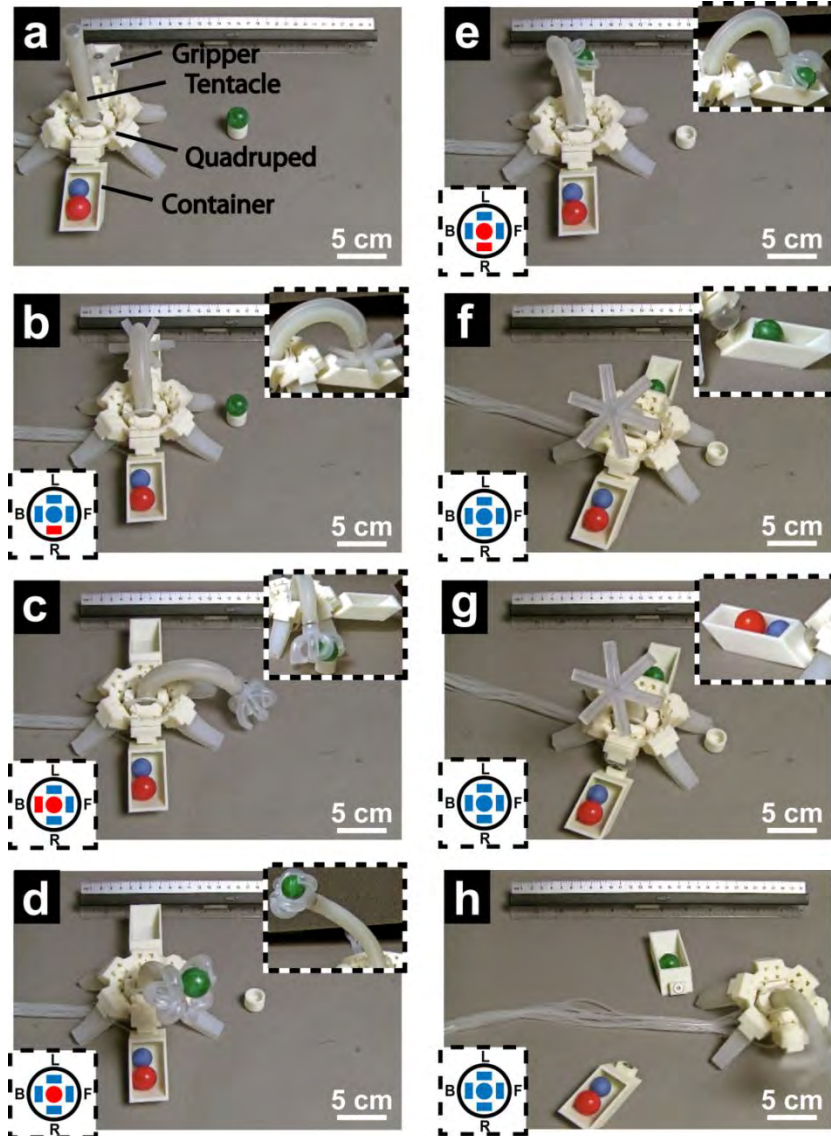


**Figure 37.** Self-alignment of ring magnets enabled remote assembly of soft actuators, and connection of pneumatic channels for actuation of a soft-hard porter. Panels a-h show the top perspective view of the robot. Insets at the bottom left corner of panels b-h show the state of actuation of side and central channels of the soft tentacle. The colored circle at the center represents the central channel while each colored rectangle represents one of the four side channels of the soft tentacle. Non-actuated states are blue while actuated states are red. Notations F, B, R, L denote the front, back, right, and left of the robot. Insets at the top right corner of panels b-g show the expanded front view of the robot. (a) A pneumatically actuated quadrupedal porter moved towards its target (green sphere). (b) Pneumatically actuated soft tentacle positioned its apex to connect a soft gripper embedded with a ring magnet. (c-e): The assembled

tentacle-gripper picked up, and placed the green sphere into the left container for transport. (f, g): After moving forward for a short distance, the robot stopped. Actuations of the inflatable adaptors unloaded the cargo together with the containers. (h): Robot continued its forward trajectory after the delivery of cargo had been completed.

## 16. SOFT ROBOTIC CAMOUFLAGE

The optical transparency of silicone rubbers provides the opportunity to change the colors of our robots. By flowing colored liquids through a “sub-dermal” microfluidic circulatory system, we dynamically altered the color of a quadrupedal soft robot (Figure 38).

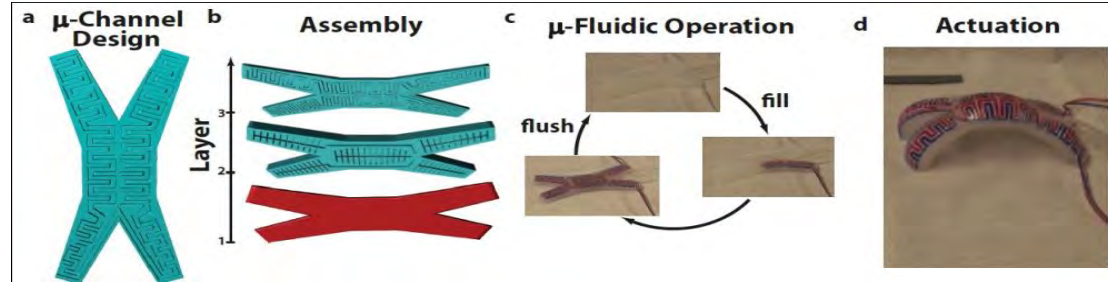


**Figure 38.** (a)  $\mu$ -Fluidic circulatory system that is (b) layered onto an existing locomotive, quadruped robot body. (c) Red/blue dyed liquids are pumped through the  $\mu$ -fluidic network, changing the skin color of the robot. (d) The  $\mu$ -fluidic network does not alter the locomotive capabilities of the robot.

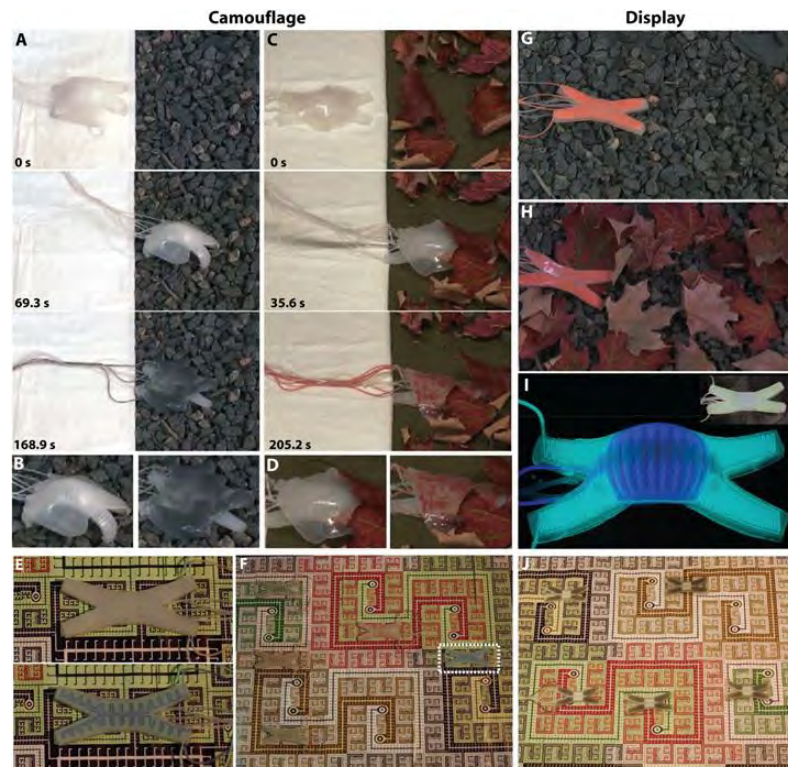


**Figure 39.** Camouflage and display coloration. (A) Sequential images of a soft robot walking onto a rock bed where it is camouflaged by pumping colored pigment dispersions through the microfluidic channels in the color layer. The number at the bottom left corner of each frame is the time (seconds). The tether is intentionally left visible to contrast the colors used against a white background. (B) Close-up images of the robot un-camouflaged (left) and camouflaged (right). (C and D) Images of a soft robot walking onto a leaf-covered concrete slab where it is camouflaged. (E) Close-up image of an un-camouflaged (top) soft robot in an artificial, man-made environment and

the same soft robot camouflaged (bottom). (F) The robot from E in five different regions adopting coloration for background matching. One position of the robot from E is marked with a dashed box; fig. S3 shows all five. (G) Fluorescent orange robot displayed on a rock bed. (H) Robot from G displayed on a leaf-covered rock bed. (I) Robot glowing in the dark using chemiluminescence (inset: the same robot photographed in the light). (J) Robots displayed in contrasting black and white on the pattern from F. All quadrupeds were 13 cm long.

## 17. HARSH ENVIRONMENT TESTING –

Our untethered soft robot body's material and monolithic design enable it to withstand a variety of harsh environmental conditions against which traditional robots must be carefully protected. This section describes experimental results that demonstrate some of the robot's capabilities.

### A. Load carrying ability

Starting from a flat position, a tethered version of the soft robot was able to lift a mass of 3.4 kg (7.5 lbs) when the legs and spine were pressurized to just below their maximum tolerances (139 kPa, 20psi). Subtracting the mass of the power and control components (1.2 kg, 2.6 lbs), this represents a net payload capacity of 2.2 kg (4.9 lbs), or 44% of the total mass of the untethered robot (Fig. 40).

Once the robot is in the standing position, the lower moment arm of a central mass on the legs meant that they could carry a larger load. With an internal pneumatic pressure of 139 kPa (20psi), the robot was able to hold a mass of 8.0 kg (17.6 lbs), or 160% of the total mass of the untethered robot.

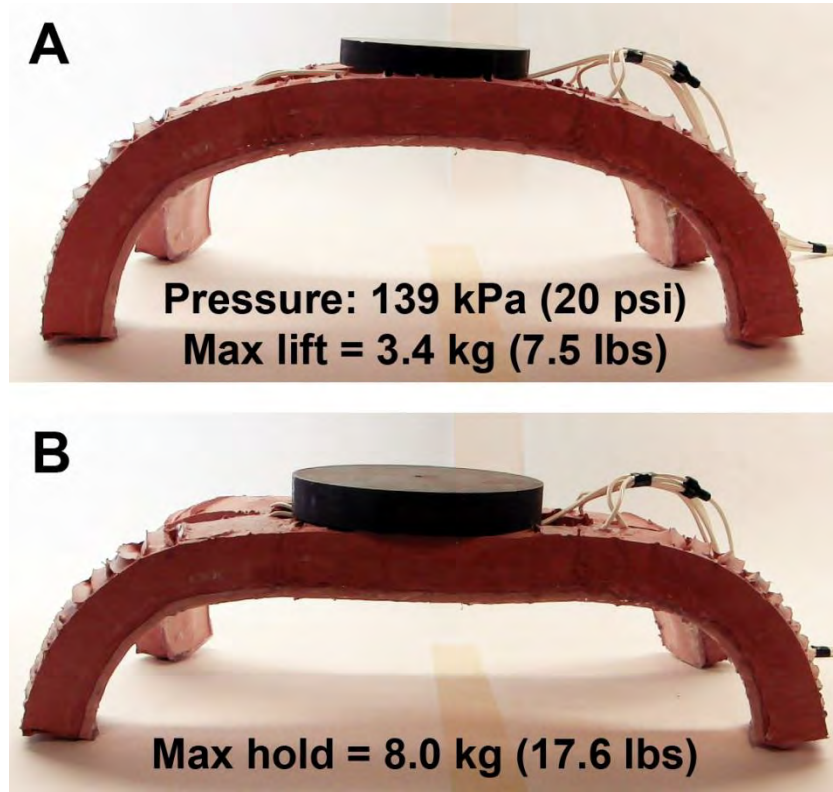


**Figure 40.** Maximum lift and hold tests. **A** Starting from a flat position, a tethered version of the soft robot was able to lift a mass of 3.4 kg (7.5 lbs) when actuated with a pneumatic pressure of 139 kPa (20psi). **B** Starting from an actuated position with an internal pneumatic pressure of 139 kPa (20psi), the robot was able to hold 8.0 kg (17.6 lbs).

## B. Survivability

As a demonstration of the ability of our untethered soft robot to withstand harsh conditions, we programmed the robot to walk under a Subaru Outback wagon in cold, wet conditions and stop with its front legs in the path of the car's tires (Fig. 41). After venting all of the robots Pneu-Nets, we drove over the soft legs. After a preprogrammed delay, the robot stood up and continued walking with no damage from the ~2000 kg (4500 lbs) vehicle, or the ambient conditions.

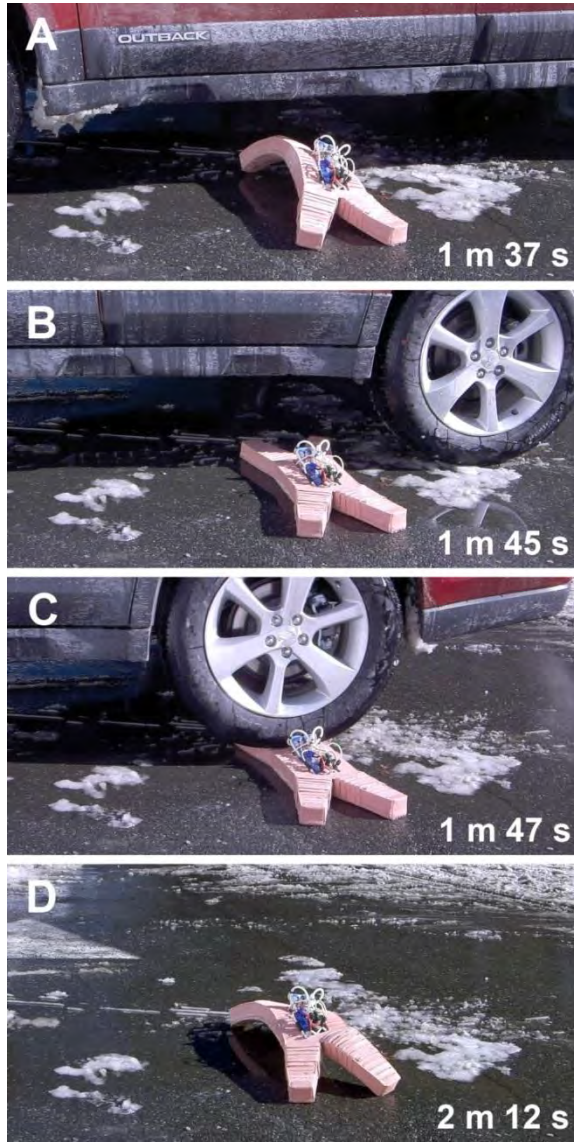


**Figure 41.** Frames from an experiment testing the soft robot's resistance to crushing force. **A** The robot ambulates underneath a Subaru Outback. **B** The robot depressurizes its actuators in preparation for impact. **C** The car running over the elastomeric legs of the soft robot. **D** The soft robot actuating and standing up after being ran over by the car.

## C. Cold weather

Our robot successfully executed its walking gait outside during a snowstorm (Nemo) with an average temperature of -9°C (15°F), and average wind speed of 40 km/h (25 mph, Fig. 42a). Because of the low

glass transition temperature of the robot's body material ( $\sim -120$  °C), as well as the lack of sliding parts (e.g. bearings) to be contaminated, the robot ambulated normally in the snow and cold weather.

#### D. Through water

Beginning on a raised platform, our robot walked down a ramp into a plastic tray filled with 5 cm (2 in) of water (Fig. 42c). The robot's body is hydrophobic and inherently sealed against water (as well as resistant to acids, thus it suffered no damage walking through water).

#### E. Through fire

We manually controlled the ambulation of a tethered version of the soft robot across metal grates through two flames (Fig. 42b). Despite the relatively long resting time of the robot in the flames during the gait ( $\sim 20$  s/cm<sup>2</sup>, though each cm<sup>2</sup> is stable to direct flame for  $\sim 60$  s), the robot suffered only superficial damage due to silicone's resistance to fire and high temperatures.

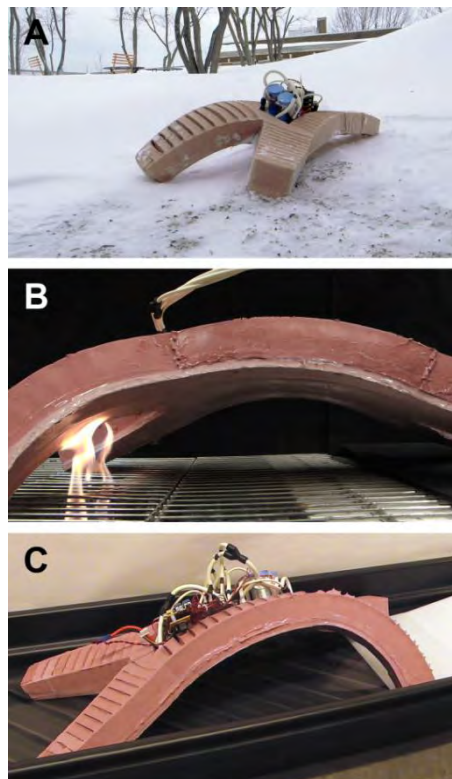


**Figure 42.** Images from experiments of our soft robot operating untethered in a variety of harsh conditions, including **A** in snow and freezing temperatures, **B** in flames, **C** in liquid.

## 18. UNDULATION LOCOMOTION ON SOFT, SLIPPERY & GRADED TERRAIN

The PneuNets robot has three individually addressable segments – by actuating them sequentially, back to front, we cause the robot to locomote in an undulation gait. Simulations revealed that, depending on terrain properties, the actuation sequence must be altered to drive the robot forward.

If the body of the robot interacts strongly with the terrain and the feet of the robot do not, undulation causes the robot to drive forward (Figure 43 a,b). Conversely, if the feet of the robot strongly interact with the terrain and the body does not, the robot drives in the reverse direction (Figure 43 c,d). Using these simulations as guidelines, we experimentally determined two classes of terrain that match these parameters: hard surfaces with moderate shear adhesion forces (wood, fabric, etc.; Figure 43 b) and soft surfaces with little shear adhesion force (wet gelatin; Figure 43 d).

The low pressure generated by the robot (it is low density and the gait uses a large contact area) allows it to traverse the soft terrain in Figure 43d: the feet of the robot can dig into the surface of the gelatin (~ 1 kPa modulus) without permanently damaging it. Also, the large contact area, during most of the

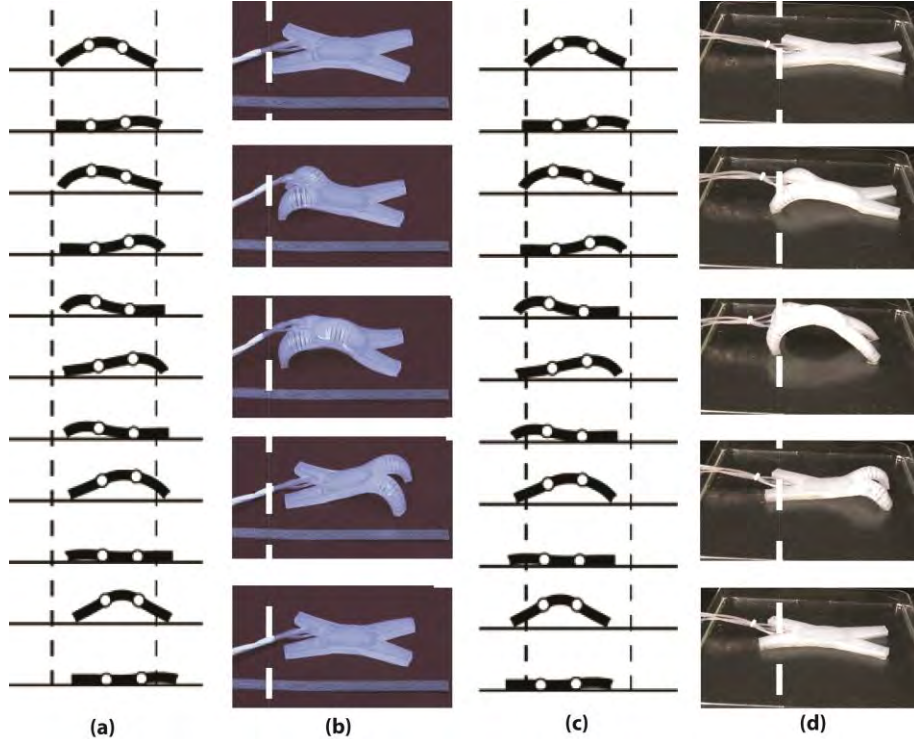


**Figure 43.** (a) Simulation and (b) experiment, where the body interacts strongly with the surface and the feet are free to slide. The surface in (b) is felt fabric. (c) Simulation and (d) experiment where the body is free to slide and the feet interact strongly with the surface. The surface in (d) is wet gelatin.

undulation gait, allows the robot to grip and, thus, locomote on slippery surfaces. The physical properties of the robot, the grip of the undulation gait, and our new knowledge of terrain interaction allowed us to drive the robot on a simulated muddy hill (Figure 44).

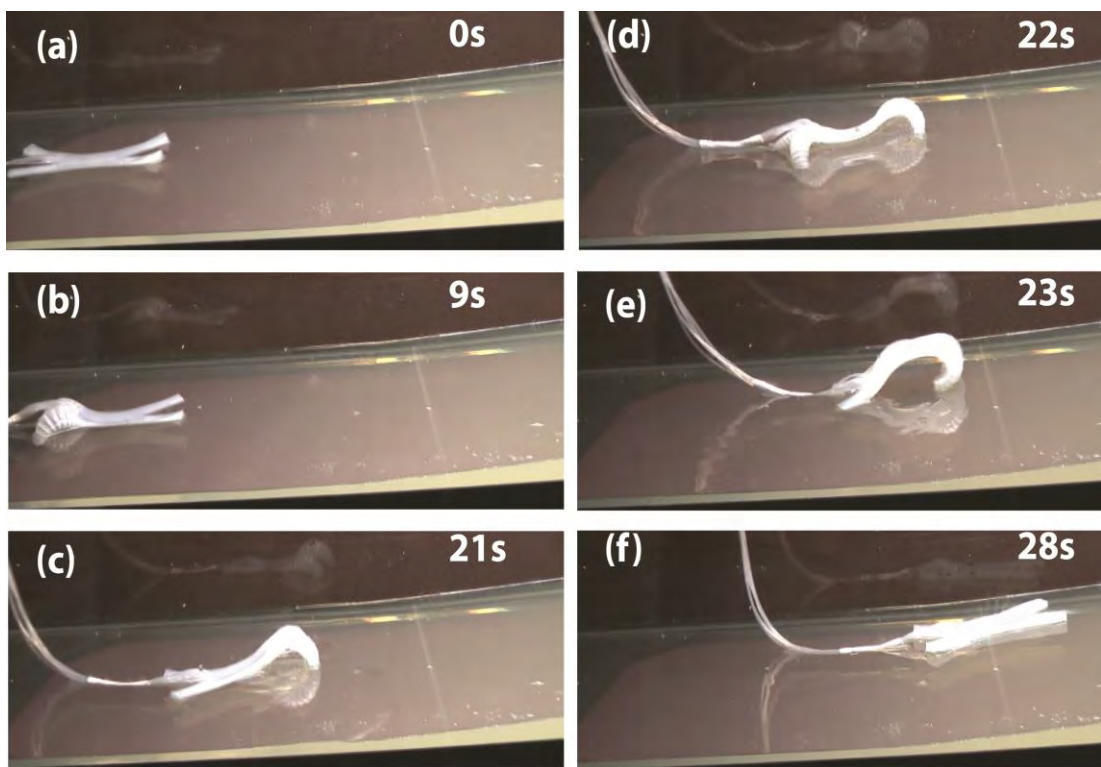


**Figure 44.** (a,b) The robot floats in a shallow volume of water onto (c-f) a  $\sim 15^\circ$  gradation of wet gelatin. [the timestamp during this locomotive sequence is indicated in the top-right]

## 19. A HYBRID COMBINING HARD AND SOFT ROBOTS

We've developed a hybrid robotic system combining hard and soft subsystems. This hybrid comprises a wheeled robot (an iRobot Create; hard) and a four-legged quadruped (soft) (Fig. 45). It is capable (using a simple, wireless control system) of rapid locomotion over flat terrain (using the wheeled hard robot) and of gripping and retrieving an object (using the independent locomotive capabilities of the soft robot). The utility of this system is demonstrated by performing a mission requiring the capabilities of both components: retrieving an object (iPod Nano) from the center of a room (Fig. 46).

Using a die-cutting machine (Silhouette Cameo) we created paper origami-carbon ink bump sensors (Fig. 47). The control system measures the resistance of the carbon ink in the sensors—this resistance changes as a function of the angle of flex at the hinge<sup>21</sup>—and uses the measurement to determine if the robot needs to change course. The bump-sensors show proof of concept in allowing the robot to move reactively—it can alter its course due to interaction with an object, such as a wall. The total cost of the control system is approximately \$150; the robot, plus sensor network, costs approximately \$5.

This class of robot—hybrids comprising hard and soft systems functioning synergistically—is capable of performing tasks that neither can do alone. In contrast to specialized hard robotic arms with grippers (capable of performing some of the functions we describe here), which are complex, relatively expensive, and require sophisticated controls, this hybrid system is easy to construct, simple to control, and low in cost. The soft robotic system in the hybrid is lightweight, disposable if contaminated or damaged, and capable of multiple functions.

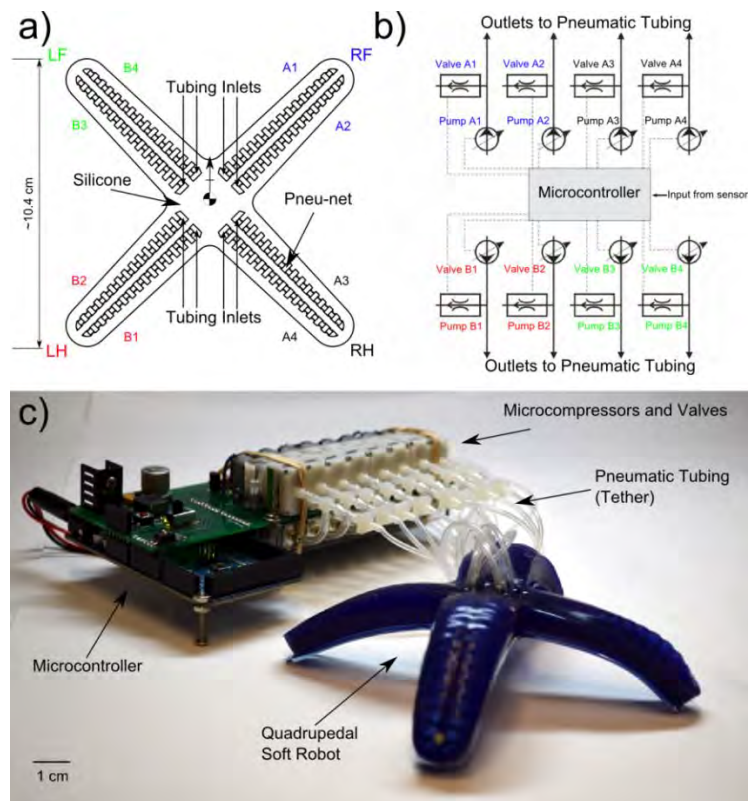


**Figure 45.** A photograph of the hybrid robotic platform showing the wheeled hard robot (iRobot Create©) and the legged soft robot. The hard robot carried, in marsupial fashion, the legged soft robot, the electro-pneumatic control system, and the wireless communications system. This figure does not show the wireless camera that was mounted on the hard robot.

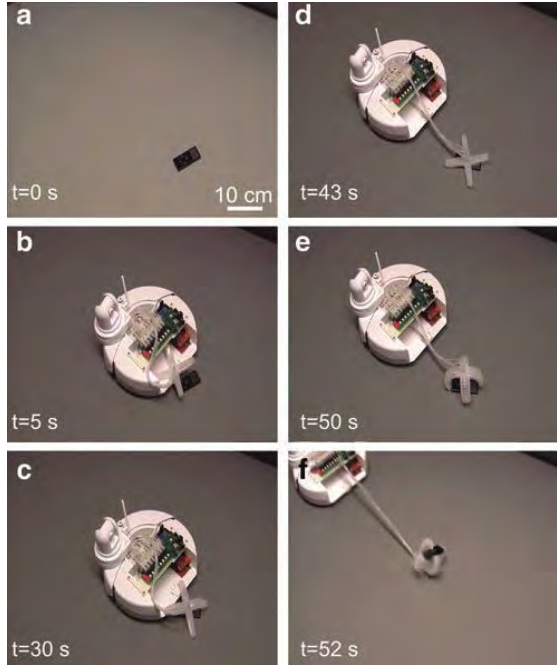


**Figure 46.** A series of still-frames show the hybrid robotic system retrieving an object (iPod Nano®) from the centre of a room (a-f). The hard robot carries the soft robot to the object (b). The soft robot, first acts as a walker (c-d), and then as a gripper (e). When the hard robot is driven away (f), the soft robot inverts, and protects the iPod as it is pulled to a new location.

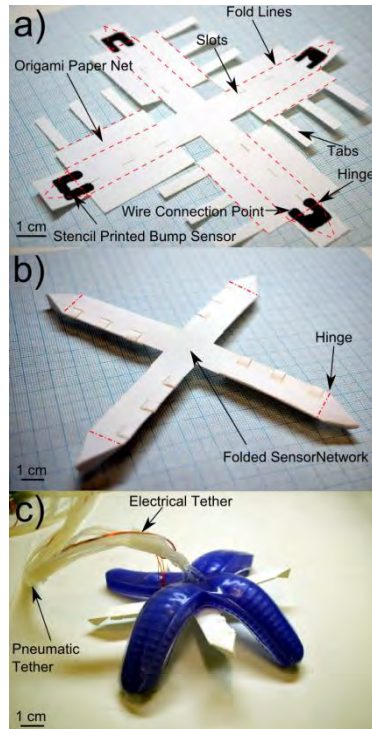


**Figure 47.** a) Design of the net for the paper-MEMS based bump sensors. Stencil-printed carbon ink patches are used as piezoresistive sensors. Copper wires (not shown) are connected to the sensor using silver epoxy. b) The folded form of the sensor network showing the triangular cross section of the arm and the top-side of the flexible hinge containing the piezo sensor. c) Photograph of the soft robot with the sensor array mounted on the underside. Both the sensor network and the robot measure 15 cm from point to point through their centers.